nature medicine

Article

https://doi.org/10.1038/s41591-026-04740-9

Neoadjuvant nivolumab with or without visugromab in muscle-invasive bladder cancer: the phase 2a GDFATHER-NEO trial

Received: 7 September 2026

Accepted: 6 October 2026

Published online: 24 October 2026

Check for updates

A list of authors and their affiliations appears at the end of the paper

Growth differentiation factor-15 (GDF-15) is overexpressed in muscle-invasive bladder cancer (MIBC) and was recently identified as a potential therapeutic target to overcome resistance to programmed cell death protein 1/programmed death ligand 1 (PDL1) blockade. We investigated the safety and efficacy of GDF-15 blockade in an exploratory, stratified, placebo-controlled, single-blinded, nonrandomized phase 2a trial (GDFATHER-NEO). Thirty-one cisplatin-ineligible or cisplatin-refusing patients with newly diagnosed MIBC (clinical T2–T4aN0M0) were stratified by tumor stage and PDL1 combined positive score (CPS) and allocated sequentially to receive three cycles of neoadjuvant nivolumab (N, 480 mg 4-weekly) plus the GDF-15-neutralizing antibody visugromab (V, 20 mg kg^{-1} 4-weekly; $n = 16$) or placebo (P, $n = 15$), followed by radical cystectomy or repeat transurethral resection of the bladder tumor. Locally assessed pathologic complete response (pCR, ypT0N0/x) and Response Evaluation Criteria in Solid Tumors v1.1-based radiographic response served as dual primary endpoints. pCR was 33% (5 of 15, 95% confidence interval (CI) 12–62%) in patients receiving N + V versus 8% (1 of 13, 95% CI 0–36%) for N + P; major pathologic response was 60% (95% CI 32–84%) versus 23% (95% CI 5–54%), and radiographic overall response rate was 60% (95% CI 32–84%) versus 15% (95% CI 2–45%), respectively. Responses to N + V were associated with higher baseline densities of total and proliferating (Ki-67^{+}) $CD8^{+}$ T cells, but independent of CPS and baseline GDF-15 levels in serum and tumor. There were no treatment-related discontinuations or treatment-related delays to surgery; grade 3–4 treatment-related adverse events occurred in two (13%) and three (20%) patients treated with N + V or N + P, respectively. These findings support further evaluation of visugromab in MIBC. ClinicalTrials.gov identifier: NCT06059547.

e-mail: necchi.andrea@hsr.it

Bladder cancer is the ninth most commonly diagnosed cancer worldwide, with globally more than 600,000 new cases and approximately 220,000 deaths estimated for 2022 and a male-to-female ratio of about 3:1 (ref. 1). Around 75% of patients present with non-muscle-invasive bladder cancer (NMIBC). Most patients with muscle-invasive (≥T2) bladder cancer (MIBC) present with primary invasive disease, whereas up to 15% had progressed from NMIBC, almost exclusively from high-risk disease[2].

The treatment of MIBC is at a watershed moment: novel, more effective systemic therapies are enabling an increasing number of patients to achieve clearance of the bladder tumor and improved survival compared with the therapies that, until recently, were the only standard-of-care options[3]. This change is the culmination of a 10-year evolution of systemic therapy in MIBC, beginning with immune checkpoint inhibitor (ICI) monotherapy trials[4,5], then exploring various combination regimens[6], ultimately resulting in the regulatory approval of durvalumab plus gemcitabine–cisplatin, followed by cystectomy and adjuvant durvalumab, and of enfortumab vedotin plus pembrolizumab (EVP), on the basis of pivotal phase 3 trials[7–9]. These advances have been paralleled by profound innovation in the monitoring of treatment response, in particular the assessment of minimal residual disease using circulating tumor DNA or urinary tumor DNA[10,11].

ICIs, predominantly antibodies directed against programmed cell death protein 1 (PD-1) or programmed cell death ligand 1 (PD-L1), have entered routine practice for neoadjuvant cancer treatment since 2020[12]. In the neoadjuvant and perioperative setting, more than 30 prospective trials in MIBC have been reported since 2016[13]. These trials sought to increase the rate of pathologic complete response (pCR), an established surrogate endpoint in neoadjuvant MIBC trials[14], and to provide options for the estimated ≥50% of patients with MIBC who are ineligible for neoadjuvant cisplatin-based chemotherapy[3,13].

Neoadjuvant immune checkpoint blockade can downsize tumors, may render initially unresectable tumors resectable and may enable surgical deescalation with organ preservation[12]. Two cycles of atezolizumab[4] or three cycles of pembrolizumab[5] produced pCR rates of 31% and 37%, respectively, and the addition of ipilimumab to nivolumab (N) resulted in a pCR rate of 46%[15]. Despite this progress, more than half of all patients still do not achieve a pathologic response, opportunities for safe bladder preservation remain rare and effective, well-tolerated options for patients who are ineligible for or decline cisplatin stay limited.

Growth differentiation factor-15 (GDF-15) is a member of the transforming growth factor-β superfamily with established roles in pregnancy and tissue stress response. GDF-15 is overexpressed in many cancers, including bladder cancer, and was identified as a potent local immunosuppressant and T cell repellent and as a determinant of resistance to PD-1 and PD-L1 blockade[16,17]. Neutralization of GDF-15 is therefore a rational strategy to restore T cell infiltration and antitumor immunity.

In the first-in-human trial GDFATHER-01, the GDF-15-neutralizing antibody visugromab (V) combined with nivolumab showed antitumor activity and a favorable safety profile in patients whose tumors were refractory to or had relapsed on ongoing PD-1 or PD-L1 blockade, including advanced/metastatic urothelial carcinoma (UC)[18]. The overall response rate (ORR) in UC was 18.5% (95% confidence interval (CI) 6.3–38.1%) with a median duration of response of 28.8 months (95% CI 7.4–39.4 months)[19]. Here we report the primary results of GDFATHER-NEO, an exploratory phase 2a trial of neoadjuvant nivolumab combined with visugromab or placebo in patients with MIBC.

Results

Patient characteristics, treatment and trial design

Between 26 September 2023 and 26 March 2025, 50 patients were screened and 31 enrolled in GDFATHER-NEO at four centers in Italy. All had newly diagnosed MIBC of clinical stage T2–T4a disease; 19 of 31 (61%) had cT2 N0 M0 tumors. Twenty-two (71%) were male and 9 (29%) were female, consistent with the sex distribution of MIBC. High PD-L1 expression, defined as a locally assessed combined positive score (CPS) ≥10, was balanced between the two groups (8 of 15 (53%) in group A, receiving nivolumab plus placebo, and 9 of 16 (56%) in group B, receiving nivolumab plus visugromab). In total, 6 of 15 patients (40%) in group A and 5 of 16 (31%) in group B were ineligible for cisplatin because of impaired renal function or hearing loss; the remaining patients (9 of 15 (60%) and 11 of 16 (69%), respectively) declined cisplatin-based chemotherapy (Table 1).

Table 1 | Baseline patient and tumor characteristics

	N+P (*n*=15)	N+V (*n*=16)	Total (*n*=31)
Median age, years (range)	77 (55–83)	76 (42–83)	76 (42–83)
Sex, *n* (%)			
Female	5 (33.3)	4 (25)	9 (29)
Male	10 (66.7)	12 (75)	22 (71)
ECOG-PS, *n* (%)			
0	12 (80)	14 (87.5)	26 (83.9)
1	3 (20)	2 (12.5)	5 (16.1)
Tumor T stage at enrollment, *n* (%)			
T2	9 (60)	10 (62.5)	19 (61.3)
T3/T4a	6 (40)	6 (37.5)	12 (38.7)
PD-L1 expression, *n* (%)			
CPS ≥10	8 (53.3)	9 (56.3)	17 (54.8)
CPS <10	7 (46.7)	7 (43.8)	14 (45.2)
Tumor histology, *n* (%)			
Pure urothelial carcinoma	14 (93.3)	13 (81.3)	27 (87.1)
Mixed histology	1 (6.7)	3 (18.8)	4 (12.9)
NACC ineligibility, *n* (%)	6 (40)	5 (31.3)	11 (35.5)
Kidney function	6 (40)	4 (25)	10 (32.3)
Hearing loss	0	1 (6.3)	1 (3.2)
Patient refusal, *n* (%)	9 (60)	11 (68.8)	20 (64.5)
Baseline lesions per RECIST, *n* (%)			
Measurable target lesion	14 (93.3)	10 (62.5)	24 (77.4)
Nontarget lesion only	1 (6.7)	5 (31.3)	6 (19.4)
No lesion (not efficacy-evaluable)	0	1 (6.3)	1 (3.2)

ECOG-PS, Eastern Cooperative Oncology Group performance status; N+P, nivolumab plus placebo; N+V, nivolumab plus visugromab; NACC, neoadjuvant cisplatin-based chemotherapy.

Within strata defined by clinical tumor stage and locally assessed PD-L1 expression, patients were allocated sequentially to three 4-weekly cycles of intravenous nivolumab 480 mg plus placebo (group A) or to three cycles of nivolumab 480 mg plus visugromab 20 mg kg^{-1} infused before nivolumab (group B); patients were blinded to their allocation (Fig. 1b). Four to eight weeks after the last dose, patients were restaged by imaging (that is, cross sectional imaging with thorax–abdomen computed tomography (CT) scan, with or without pelvic magnetic resonance imaging (MRI) scans) and underwent radical cystectomy (RC). Those who refused RC were offered the option to receive a repeat transurethral resection of the bladder tumor (re-TURBT) within a multidisciplinary tumor board discussion and after careful discussion with the patients. Surgery was followed by observation alone or by additional off-protocol therapy at the investigator's discretion.

The two primary endpoints were the rate of pCR (defined as ypT0 N0 or ypT0 NX, depending on the type of surgery received) and the rate

https://doi.org/10.1038/s41591-026-04740-9

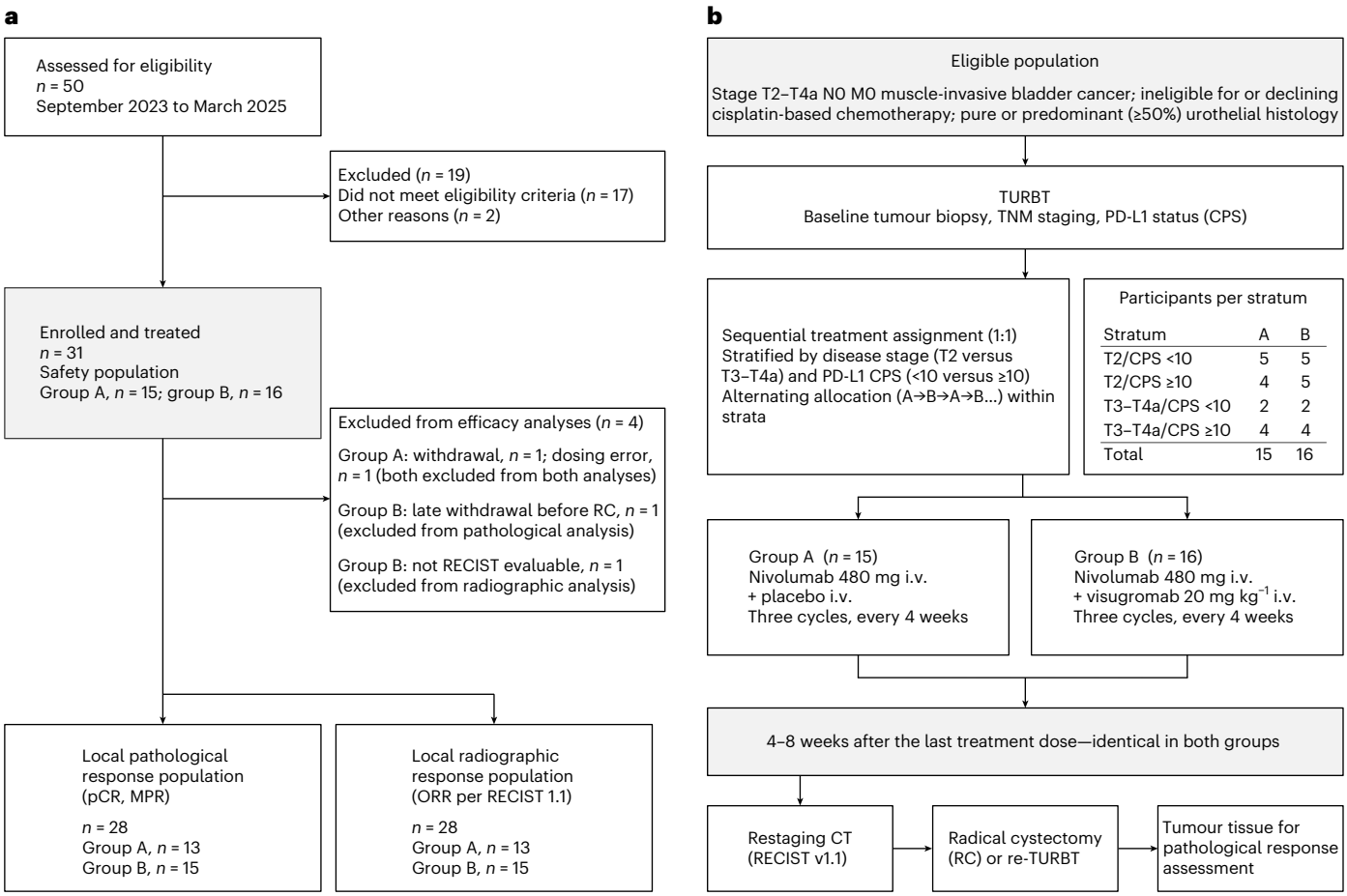


Fig. 1 | GDFATHER-NEO trial design and CONSORT flow diagram. a, CONSORT diagram showing the flow of participants in the GDFATHER-NEO trial in which histopathologic response and radiographic response (per RECIST v.1.1) were both assessed to evaluate the efficacy of this multimodal treatment approach. **b**, Design of the covariate-stratified, parallel-group comparative phase 2a trial with sequential treatment allocation within strata. i.v., intravenous.

of radiographic response according to Response Evaluation Criteria in Solid Tumors (RECIST) version 1.1, both by local assessment (Fig. 1a). Secondary endpoints comprised major pathologic response (MPR), defined as ypT0/Ta/Tis/T1 N0 after RC (or Nx after re-TURBT), centrally assessed pathologic and radiographic response, time-to-event endpoints including event-free survival (EFS), pharmacokinetics and safety.

Of the 31 patients in the safety analysis population, which was identical to the intention-to-treat population, three patients (two in group A and one in group B) stopped neoadjuvant treatment after the first cycle owing to adverse events (AE), and 28 patients (13 in group A and 15 in group B) received all three planned cycles (Extended Data Table 1). Nine of 31 patients (29%) underwent re-TURBT (3 in group A and 6 in group B), 1 of whom (group B) subsequently underwent RC, and 19 (61%) underwent RC alone (10 in group A and 9 in group B). Three patients did not undergo protocol-defined surgery: two withdrew consent before surgery, and one discontinued neoadjuvant treatment early and underwent RC outside the trial. Adjuvant therapy was given to five patients, all in group A: chemotherapy in four (cisplatin plus gemcitabine in three and carboplatin plus gemcitabine in one) and radiotherapy after TURBT in one.

Protocol deviations mostly concerned missing laboratory assessments and deviations from protocol-defined time windows for participants' clinical visits. In five participants, retrospective analysis showed that not all eligibility criteria were met; in two participants, investigational medicinal product administration errors occurred leading to the exclusion of one participant from all efficacy analyses; in two participants, re-TURBT had been conducted instead of radical cystectomy before formal introduction of this option with a respective protocol amendment.

Five patients received chemotherapy for recurrent disease: three in group A (carboplatin plus gemcitabine in two and carboplatin followed by carboplatin plus gemcitabine in one) and two in group B (cisplatin plus gemcitabine in both, followed by avelumab in one).

Pathologic and radiographic response

Twenty-eight patients were evaluable for locally assessed pathologic response and 28 for locally assessed radiographic response (Fig. 1a). In group A, one patient withdrew consent before the protocol-defined primary endpoint assessment and one received an incorrect dose; both were excluded from the pathologic and the radiographic efficacy analyses, leaving 13 evaluable patients for each endpoint. In group B, 1 patient who withdrew consent after response imaging but before surgery was excluded from the pathologic efficacy analysis, and a different patient with no lesion suitable for RECIST assessment by local review was excluded from the radiographic efficacy analysis, leaving 15 evaluable patients for each endpoint.

For central review, 27 patients were evaluable for pathologic response and 28 for radiographic response. In addition to the exclusions described above, one patient in group A was not evaluable for central pathologic response because no specimen was available (group A, $n = 12$; group B, $n = 15$). For central radiographic response, one patient in group A had no lesion suitable for RECIST assessment, whereas the above-mentioned patient in group B who was considered nonevaluable

by local review was considered evaluable for central review (group A, $n = 12$; group B, $n = 16$).

Among the 28 patients evaluable for locally assessed pathologic response, pCR was reached by 1 of 13 patients (8%, 95% CI 0–36%) in group A and by 5 of 15 patients (33%, 95% CI 12–62%) in group B (Fig. 2a). An additional two patients in group A and four in group B had residual ypTa, ypTis or ypT1 N0, resulting in MPR rates of 3 of 13 (23%, 95% CI 5–54%) with nivolumab plus placebo and 9 of 15 (60%, 95% CI 32–84%) with nivolumab plus visugromab.

Central pathologic review was largely concordant with local assessment, with pCR in 2 of 12 patients (17%, 95% CI 2–48%) in group A and 7 of 15 (47%, 95% CI 21–73%) in group B, and MPR in 4 of 12 (33%, 95% CI 10–65%) and 9 of 15 (60%, 95% CI 32–84%), respectively, among the 27 evaluable patients (Fig. 2b). Pathologic response rates were higher with nivolumab plus visugromab in each T stage and centrally assessed PD-L1 CPS subgroup, although the subgroups were small (Fig. 2c). Pathologic ypTNM stages for individual patients are provided in Extended Data Table 1.

By local RECIST version 1.1 assessment, two partial responses were recorded in group A (ORR 2 of 13; 15%, 95% CI 2–45%) and seven complete and two partial responses in group B (ORR 9 of 15; 60%, 95% CI 32–84%); the complete response rate was 47% (95% CI 21–73%) (Fig. 2d). Radiographic and pathologic responses were broadly concordant. Central review recorded an ORR of 4 of 12 (33%, 95% CI 10–65%) in group A and of 8 of 16 (50%, 95% CI 25–75%), including two complete responses (13%, 95% CI 2–38%), in group B (Fig. 2e). Baseline and post-treatment CT images from a patient with a radiographic and pathologic complete response by local assessment are shown in Fig. 2f.

Representative haematoxylin and eosin (H&E)-stained sections illustrate the histopathological responses observed after nivolumab plus visugromab treatment (Fig. 2g). While residual viable tumor remained in the participant who achieved MPR (even if only in the form of carcinoma in situ), no residual viable tumor was identified in the post-treatment specimen from the participant who achieved pCR.

Among radiographically evaluable participants, progressive disease as best overall response was recorded in four patients (two in each group). Two of these—one per group—had stopped neoadjuvant treatment early because of AEs (Extended Data Table 1) but were, in line with the statistical analysis plan, imputed as nonresponders.

Event-free survival

At the time of the data cutoff (15 July 2026), the median follow-up was 15.7 months ((interquartile range 15.1–16.5 months).

Event-free survival was defined as the time from cycle 1 day 1 (C1D1) to local (intravesical in patients undergoing re-TURBT) or distant recurrence documented by cross-sectional imaging and/or biopsy, to the start of therapy for progression or recurrence, or to death from any cause. Patients without an event were censored at the start of adjuvant therapy or at last follow-up.

Six events were recorded in total, three in each group. Median EFS was not reached in either group, with protocol-defined follow-up limited to 1 year after surgery (Extended Data Fig. 1; intention-to-treat population, $n = 31$). No event occurred among patients with a pCR, including the four patients in group B who underwent re-TURBT alone without subsequent RC. All six events occurred either in patients with a pathologic nonresponse or in patients who did not proceed to protocol-defined surgery. Given the small number of events and the short follow-up, these data are descriptive only. Figure 3 displays the core treatment period, surgical procedures, histopathological responses, follow-up including systemic treatments outside of the protocol-defined treatment and potential recurrence of all 31 trial participants in both groups.

Baseline CD8$^+$ T cell state and pathologic response

Baseline intratumoral immune-cell densities and phenotypes did not differ significantly between the two treatment groups (Extended Data Fig. 2), although median densities of total T cells, CD8$^+$ T cells and proliferating CD8$^+$Ki-67$^+$ T cells were numerically higher in group B (Fig. 4a). The proportion of proliferating CD8$^+$ T cells within the total CD8$^+$ T-cell compartment did not significantly differ between the treatment groups (Fig. 4a).

When T cell densities were analyzed according to pathologic response, patients showing any MPR (including patients with a pCR) to nivolumab plus visugromab had higher baseline densities of total CD8$^+$ T cells and proliferating CD8$^+$Ki-67$^+$ T cells than nonresponders ($P = 0.008$ and $P = 0.003$). No such association was observed for pathologic responders versus nonresponders in the nivolumab plus placebo group (Fig. 4b). Responses to the combination occurred across the range of centrally assessed CPS values, and PD-L1 expression did not distinguish pathologic responders from nonresponders (Fig. 4c).

These exploratory data suggest that a preexisting proliferative CD8$^+$ T cell state, rather than PD-L1 status, is associated with response to combined GDF-15 and PD-1 blockade in a rather short-term, 12-week treatment setting.

Baseline circulating total GDF-15 concentrations and intratumoral GDF-15 H scores were comparable between the two groups and were not associated with baseline densities of total T cells, CD8$^+$ T cells or proliferating T cell populations (Extended Data Fig. 3c), nor with pathologic response in either group (Extended Data Fig. 3a,b). Baseline GDF-15 abundance alone therefore did not predict baseline immune cell infiltration or treatment response in this cohort.

GDF-15 blockade has previously been associated with induction of interferon (IFN) signaling and of the IFN-inducible chemokines C–X–C motif chemokine ligand (CXCL)9 and CXCL10[18]. Circulating cytokine and chemokine concentrations were therefore assessed. Baseline concentrations of CXCL9, CXCL10 and IFN-γ were comparable between groups (Extended Data Fig. 4a). On-treatment CXCL9 and IFN-γ concentrations were frequently below the lower limit of quantification, precluding a robust assessment of treatment-associated changes, whereas longitudinal CXCL10 concentrations varied substantially between patients without a consistent difference between groups (Extended Data Fig. 4b).

Taken together, in this neoadjuvant setting, baseline infiltration with proliferating CD8$^+$ T cells appears to correlate with response to

Fig. 2 | Histopathologic and radiographic response and correlation between endpoints and with strata. a, Locally assessed histopathologic response (pCR and MPR) per treatment group. **b**, Centrally assessed histopathologic response (pCR and MPR) per treatment group. **c**, Correlation of histopathologic response by local (upper line) and central (lower line) assessment with tumor stage (T2 versus T3–T4a) and PD-L1 expression (CPS ≥10 versus CPS <10, central assessment; one participant in the N + P group was not evaluable for central CPS score). **d**, Locally assessed radiographic response (RECIST v.1.1) per treatment group and its correlation with local histopathologic response. **e**, Centrally assessed radiographic response (RECIST v.1.1) per treatment group and its correlation with central histopathologic response. **f**, CT images from one participant illustrative of depth of response achieved after three cycles of neoadjuvant treatment with combined nivolumab plus visugromab. **g**, Representative haematoxylin and eosin (H&E)-stained sections from participant 19, who achieved an MPR, and participant 12, who achieved a pCR. For each participant, baseline (left) and post-therapy specimens (right) are shown. For participant 19, arrows indicate confluent tumor zones with variable tumor cell types at baseline and T1 tumor after therapy. For participant 12, the arrow indicates tumor cells invading the muscularis, whereas no residual viable tumor was detectable post-therapy. Scale bars, 200 µm. H&E staining was performed once per specimen as part of central pathology review; images are from representative patients with MPR and pCR. ITT, intention to treat; NE, nonevaluable; pNR, pathological nonresponse.

https://doi.org/10.1038/s41591-026-04740-9

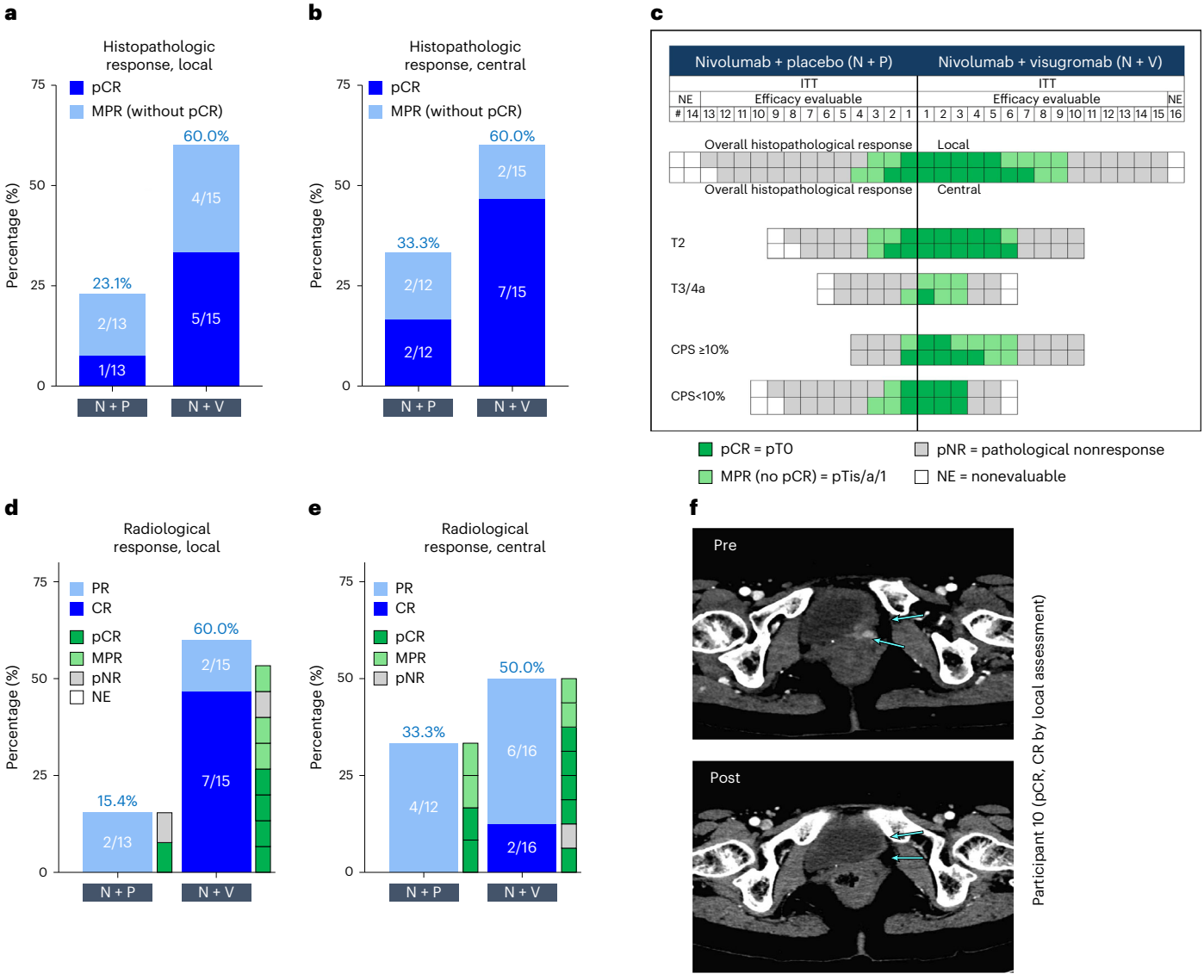
nivolumab plus visugromab, whereas baseline GDF-15 abundance or PD-L1 expression seem to be nonpredictive.

Pharmacokinetics

Total visugromab serum concentrations were similar across treated patients and consistent with those observed in the first-in-human GDFATHER-01 phase 1/2 trial (Extended Data Fig. 5). Mean serum concentrations declined between dose administrations but remained above 100 μg ml^{-1} during the 4-week intervals, consistent with continued GDF-15 neutralization over the whole treatment period.

Safety

The safety analysis population comprised all 31 patients who received at least one dose of trial treatment (Table 2 and Extended Data Table 2).



https://doi.org/10.1038/s41591-026-04740-9

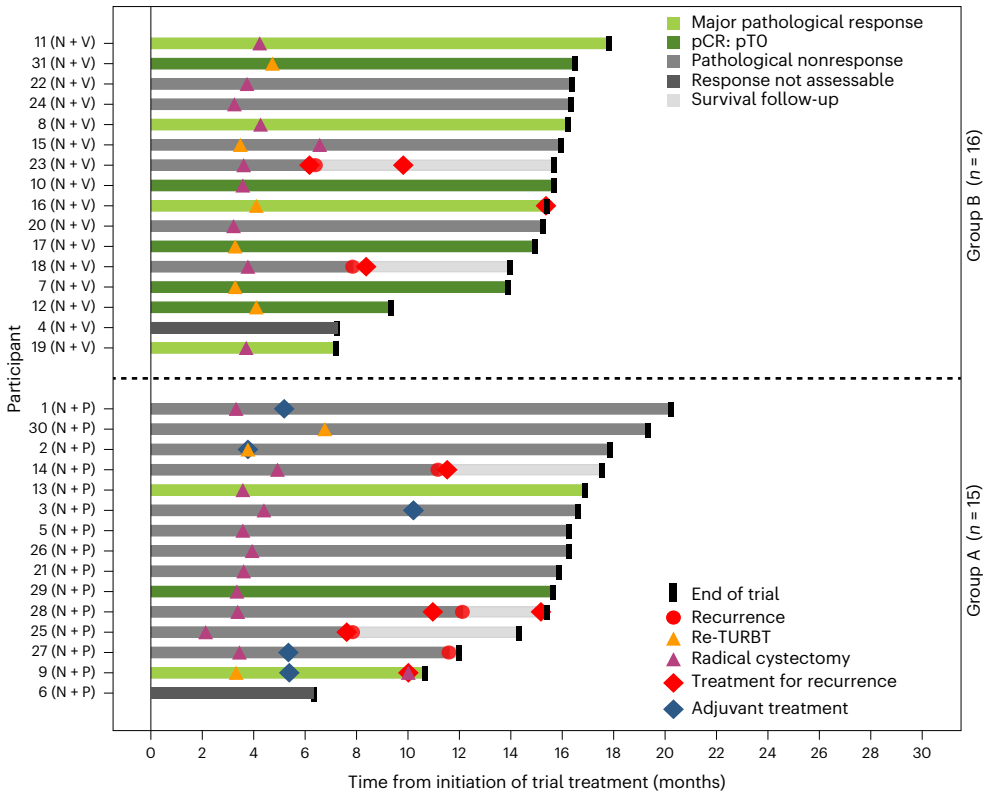


Fig. 3 | Follow-up data for trial participants. Swimmer plots for all 31 trial participants across both treatment arms, depicting all surgical interventions, the local histopathologic response, systemic treatment outside of the trial treatment and disease recurrence occurring during the core trial period and the follow-up period. End-of-trial visit for participant 25 was confirmed post data cutoff (15 July 2026).

AEs of any grade were recorded in every patient. No treatment-related deaths occurred. One patient in group A died from disease progression, approximately 9 months after RC.

Grade 3–4 treatment-emergent AEs (TEAEs) were reported in 20 of 31 patients (65%): 12 of 15 (80%) in group A and 8 of 16 (50%) in group B (Extended Data Table 2). Treatment-related AEs (TRAEs) of any grade were more frequent with nivolumab plus visugromab (14 of 16 (88%) versus 8 of 15 (53%) for nivolumab plus placebo), driven mainly by asthenia, pruritus and hypothyroidism, whereas grade 3–4 treatment-related events occurred in 5 of 31 patients (16%) and were less frequent with nivolumab plus visugromab (2 of 16, 13%) than in the control group (3 of 15, 20%). These comprised increased liver transaminases in both groups, hypothyroidism and myalgia in group A and interstitial lung disease in group B; the increase in liver enzymes in group B occurred in the context of an immune-mediated hepatic disorder (Table 2). Three serious TRAEs were recorded: immune-mediated hepatic disorder and interstitial lung disease in group B, and hypothyroidism in group A.

At the preferred-term level, asthenia, pruritus and hypothyroidism were numerically more common in group B. Immune-related AEs occurred in 9 of 31 patients (29%): 4 of 15 (27%) in group A and 5 of 16 (31%) in group B; grade 3–4 immune-related events occurred in 5 of 31 patients (16%): 3 of 15 (20%) in group A and 2 of 16 (13%) in group B (Extended Data Table 3). All immune-related events except for one case of pruritus in group B required systemic treatment, with corticosteroids given in seven patients and hormone replacement only in one participant with hypothyroidism. Two patients in group A, and no patients in group B, discontinued systemic treatment because of a TRAE (Table 2).

Surgery was postponed, that is, versus the originally planned date, in five patients in group A and in six patients in group B. One delay in group A was attributed to a non-treatment-related toxicity, and one delay in each group to disease progression; all remaining delays were for logistical reasons only. No postoperative complication attributable to neoadjuvant treatment was recorded.

No relationship was detected between pharmacokinetic exposure and the occurrence of treatment-emergent AEs. One patient in group B had preexisting, transiently detectable ADAs, with no apparent effect on pharmacokinetics or clinical outcome.

Discussion

MIBC treatment has been revolutionized by the advent of enfortumab vedotin, an antibody–drug conjugate, administered in combination with the PD-1 inhibitor pembrolizumab (EVP). The combination establishes a new standard of care, with pCR rates exceeding 50% in both cisplatin-eligible and cisplatin-ineligible populations[8,9]. Identifying novel agents that are sufficiently potent and safe to be considered for further combinatorial development with EVP is a central focus of current clinical research, with one main focus on integrating well-tolerable immunotherapeutic approaches. In parallel, increasing the proportion of patients who can forgo RC through effective perioperative therapy followed by re-TURBT is an emerging paradigm under investigation in trials such as EV-209 (NCT07475806) and EV-309 (NCT07566156), and deescalation of perioperative therapy by omitting RC or the adjuvant component is a further priority. Enhancing the efficacy of the neoadjuvant component, and thereby the clinical complete response rate, would allow more patients to be considered for such deescalation.

In the exploratory GDFATHER-NEO phase 2a trial, the addition of the GDF-15-neutralizing antibody visugromab to neoadjuvant nivolumab was associated with three- to fourfold higher rates of pathologic and radiographic response than nivolumab alone in patients with MIBC who were ineligible for or who declined cisplatin-based chemotherapy. GDFATHER-NEO is the first trial to evaluate GDF-15 neutralization in the neoadjuvant setting and provides an initial estimate of the effect size of combined GDF-15 and PD-1 blockade

https://doi.org/10.1038/s41591-026-04740-9

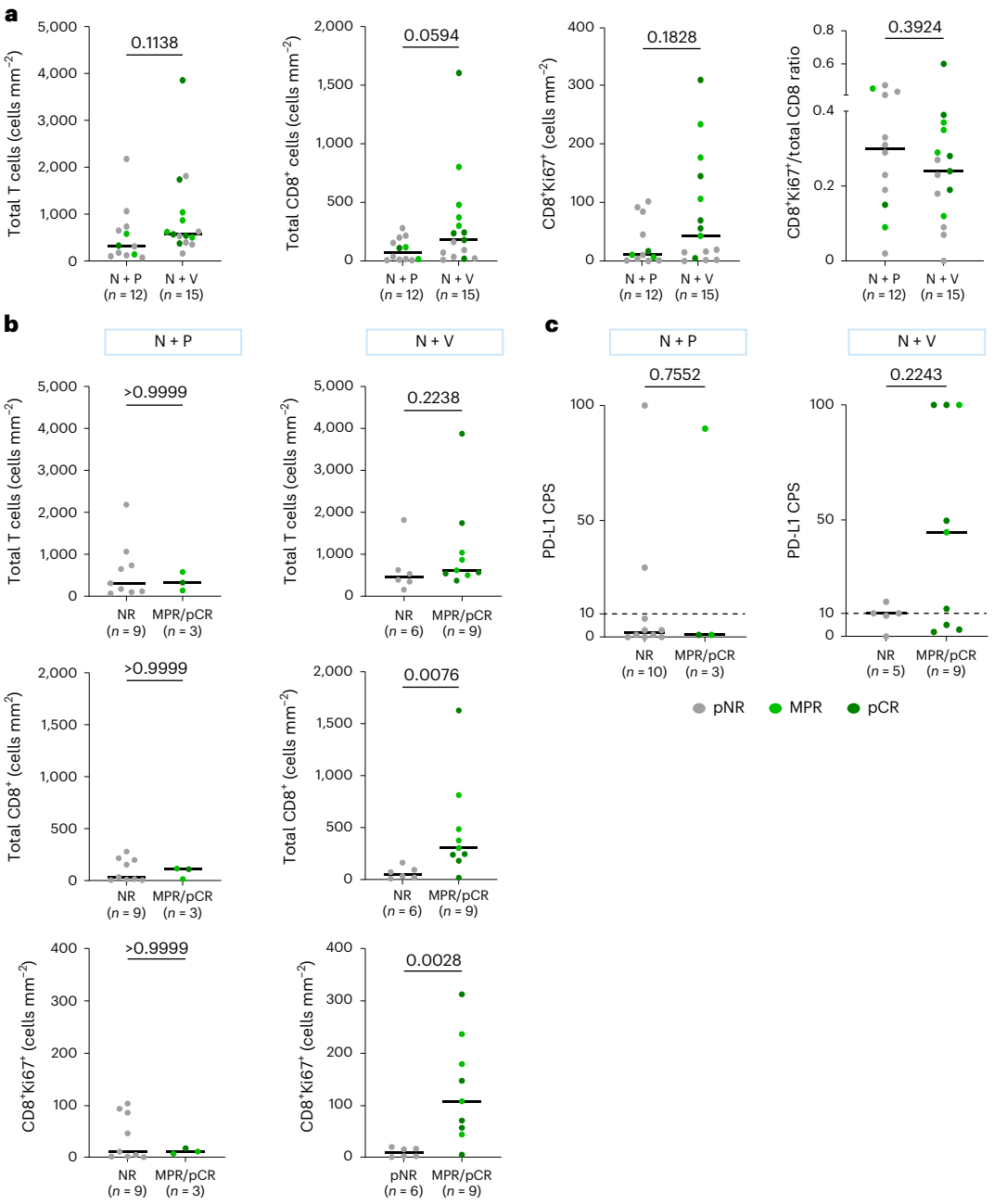


Fig. 4 | Baseline CD8⁺ T cell states identify tumors responding to combined GDF-15 and PD-1 blockade. a, Baseline densities of total T cells, total CD8⁺ T cells and proliferating CD8⁺ T cells (CD8⁺Ki67⁺) and the ratio of proliferating CD8⁺ T cells to total CD8⁺ T cells in patients treated with nivolumab plus placebo (N + P) or nivolumab plus visugromab (N + V). **b**, Baseline densities of total, CD8⁺ and CD8⁺Ki67⁺ T cells stratified by local pathologic response within each treatment group. **c**, Association of centrally assessed PD-L1 CPS with local pathologic response. The horizontal dotted line denotes the PD-L1 CPS cutoff of 10. Each data point represents one baseline tumor sample from one individual patient. No repeated measurements from the same patient were included within any statistical comparison. Horizontal lines indicate medians. The distribution of individual observations is shown. Statistical comparisons were performed using two-sided Mann–Whitney *U* tests. *n* represents individual patients with an evaluable baseline tumor sample and available biomarker measurement. mIF staining and analysis were performed once per patient specimen; each data point represents one patient. mIF, multiplex immunofluorescence; NR, no (pathologic) response.

in newly diagnosed, checkpoint-inhibitor naive, systemically previously untreated patients with bladder cancer. GDF-15 is a regulator of antitumor immunity[20], and its neutralization has been proposed as a means of reversing the immune exclusion that limits the activity of PD-1 and PD-L1 blockade. Transcriptomic analyses of approximately 10,000 tumors from The Cancer Genome Atlas and related datasets have implicated GDF-15-mediated immunosuppression across several tumor types, including urothelial carcinoma[18], and notable clinical activity of visugromab plus nivolumab has been reported in patients with urothelial carcinoma, nonsquamous non-small cell lung cancer and hepatocellular carcinoma whose disease was refractory to or had relapsed on ongoing PD-1/-L1 blockade and who had exhausted available treatment options, with observation of deep, long-term responses with the combination in a subgroup of treated patients[19].

Patients in the GDFATHER-NEO trial were stratified by clinical tumor stage and PD-L1 expression and were then allocated sequentially to nivolumab plus visugromab or to nivolumab plus matching placebo (Fig. 1b). Locally assessed pCR was 33% with the combination

https://doi.org/10.1038/s41591-026-04740-9

Table 2 | Treatment-related AEs, serious AEs and discontinuations

System organ class or preferred term	N+P (*N*=15) patients, *n* (%)		N+V (*N*=16) patients, *n* (%)		Total (*N*=31) patients, *n* (%)	
	Any grade	Grade 3–4	Any grade	Grade 3–4	Any grade	Grade 3–4
Treatment-related AEs	8 (53.3%)	3 (20.0%)	14 (87.5%)	2 (12.5%)	22 (71.0%)	5 (16.1%)
General disorders and administration site conditions	2 (13.3%)	0 (0.0%)	6 (37.5%)	0 (0.0%)	8 (25.8%)	0 (0.0%)
Asthenia	1 (6.7%)	0 (0.0%)	6 (37.5%)	0 (0.0%)	7 (22.6%)	0 (0.0%)
Investigations	3 (20.0%)	1 (6.7%)	3 (18.8%)	1 (6.2%)	6 (19.4%)	2 (6.5%)
Alanine aminotransferase increased	2 (13.3%)	1 (6.7%)	2 (12.5%)	1 (6.2%)	4 (12.9%)	2 (6.5%)
Aspartate aminotransferase increased	1 (6.7%)	1 (6.7%)	2 (12.5%)	1 (6.2%)	3 (9.7%)	2 (6.5%)
Gamma-glutamyl transferase increased	1 (6.7%)	0 (0.0%)	1 (6.2%)	0 (0.0%)	2 (6.5%)	0 (0.0%)
Skin and subcutaneous tissue disorders	1 (6.7%)	0 (0.0%)	5 (31.2%)	0 (0.0%)	6 (19.4%)	0 (0.0%)
Pruritus	1 (6.7%)	0 (0.0%)	3 (18.8%)	0 (0.0%)	4 (12.9%)	0 (0.0%)
Endocrine disorders	2 (13.3%)	1 (6.7%)	4 (25.0%)	0 (0.0%)	6 (19.4%)	1 (3.2%)
Hypothyroidism	2 (13.3%)	1 (6.7%)	4 (25.0%)	0 (0.0%)	6 (19.4%)	1 (3.2%)
Hyperthyroidism	1 (6.7%)	0 (0.0%)	1 (6.2%)	0 (0.0%)	2 (6.5%)	0 (0.0%)
Musculoskeletal and connective tissue disorders	1 (6.7%)	1 (6.7%)	3 (18.8%)	0 (0.0%)	4 (12.9%)	1 (3.2%)
Arthralgia	1 (6.7%)	0 (0.0%)	1 (6.2%)	0 (0.0%)	2 (6.5%)	0 (0.0%)
Pain in extremity	0 (0.0%)	0 (0.0%)	2 (12.5%)	0 (0.0%)	2 (6.5%)	0 (0.0%)
Myalgia	1 (6.7%)	1 (6.7%)	0 (0.0%)	0 (0.0%)	1 (3.2%)	1 (3.2%)
Blood and lymphatic system disorders	0 (0.0%)	0 (0.0%)	2 (12.5%)	0 (0.0%)	2 (6.5%)	0 (0.0%)
Anemia	0 (0.0%)	0 (0.0%)	2 (12.5%)	0 (0.0%)	2 (6.5%)	0 (0.0%)
Hepatobiliary disorders	0 (0.0%)	0 (0.0%)	1 (6.3%)	1 (6.3%)	1 (3.2%)	1 (3.2%)
Immune-mediated hepatic disorder	0 (0.0%)	0 (0.0%)	1 (6.3%)	1 (6.3%)	1 (3.2%)	1 (3.2%)
Respiratory, thoracic and mediastinal disorders	0 (0.0%)	0 (0.0%)	1 (6.3%)	1 (6.3%)	1 (3.2%)	1 (3.2%)
Interstitial lung disease	0 (0.0%)	0 (0.0%)	1 (6.3%)	1 (6.3%)	1 (3.2%)	1 (3.2%)
	Any grade		**Any grade**		**Any grade**	
Serious TRAEs	1 (6.7%)		2 (12.5%)		3 (9.7%)	
Hepatobiliary disorders	0 (0.0%)		1 (6.2%)		1 (3.2%)	
Immune-mediated hepatic disorder	0 (0.0%)		1 (6.2%)		1 (3.2%)	
Endocrine disorders	1 (6.7%)		0 (0.0%)		1 (3.2%)	
Hypothyroidism	1 (6.7%)		0 (0.0%)		1 (3.2%)	
Respiratory, thoracic and mediastinal disorders	0 (0.0%)		1 (6.2%)		1 (3.2%)	
Interstitial lung disease	0 (0.0%)		1 (6.2%)		1 (3.2%)	
	Any grade		**Any grade**		**Any grade**	
Immune-related AEs	4 (26.7%)		5 (31.3%)		9 (29.0%)	
	Any grade		**Any grade**		**Any grade**	
TRAEs leading to discontinuation	2 (13.3%)		0 (0%)		2 (6.5%)	
Investigations	1 (6.7%)		0 (0.0%)		1 (3.2%)	
Aspartate aminotransferase increased	1 (6.7%)		0 (0.0%)		1 (3.2%)	
Musculoskeletal and connective tissue disorders	1 (6.7%)		0 (0.0%)		1 (3.2%)	
Myalgia	1 (6.7%)		0 (0.0%)		1 (3.2%)	

TRAEs by MedDRA Preferred Term. Shown are preferred terms reported in ≥6.5% of patients (that is, for those terms for which events in at least two patients were reported), or with at least one grade 3–4 event. Terms in bold in the left column refer to System Organ Class terms.

versus 8% with nivolumab alone, MPR was 60% versus 23% and radiographic response was 60% versus 15% (Fig. 2). Central review confirmed the results, with the difference in pCR being even more pronounced (47% versus 17%).

This trial was small and not powered for formal comparison, so these estimates are descriptive only. Yet, the observed magnitude of the differences and their consistency across assessments provide an early indication that combined GDF-15 and PD-1 blockade can potentiate PD-1 blockade substantially in this setting, and support further evaluation of visugromab in combination with checkpoint inhibition in early stage, checkpoint inhibitor-naive disease.

With follow-up limited by protocol to 1 year after surgery, only six EFS events occurred and medians were not reached in either group, so the EFS data cannot be informative about long-term benefit. In line with the diverging pathologic response rates, adjuvant therapy was given to five patients in group A and to none in group B, which might be a potential explanation for the limited number of early events in the monotherapy group and in parallel also be reflective of the treatment

effect achieved in group B. No recurrence occurred among the four patients in group B who achieved a pCR after re-TURBT alone; although based on very small numbers, this observation is consistent with the growing interest in response-guided bladder preservation and supports the prospective evaluation of bladder-sparing strategies after visugromab-based combination therapy.

Pathologic responses were most frequent in patients with cT2 tumors and were observed across the range of PD-L1 expression (Fig. 2c). Treatment consisted of three 4-weekly cycles, and surgery was performed 4–8 weeks after the last dose. Whether a longer interval between the last dose and surgery, or additional treatment cycles, could further improve pathologic response or not cannot be determined from these data and merits prospective evaluation.

These results require careful contextualization. Neoadjuvant and perioperative immunotherapy has only recently entered MIBC treatment algorithms[3,21]. In NIAGARA, the addition of durvalumab to gemcitabine–cisplatin increased the pCR rate from 27.5% to 37.3% and improved EFS[7]. In cisplatin-eligible patients, EVP increased the pCR rate to 55.8% (KEYNOTE-B15/EV-304)[8], and in cisplatin-ineligible or cisplatin-declining patients, the companion phase 3 trial reported a pCR rate of 57.1% (KEYNOTE-905/EV-303), establishing a benchmark and an emerging standard of care in the population studied here[9]. Checkpoint inhibitor monotherapy trials, including PURE-01 and PANDORE (pembrolizumab), ABACUS (atezolizumab) and AURA (avelumab), have reported pCR rates of 29–37%[4,5,22], and combined PD-(L)1 and CTLA-4 blockade has produced pCR rates of 35% (DUTRENEO)[23] to 43–46% (NABUCCO)[15]. The pCR rate of 33% observed with nivolumab plus visugromab lies within the range reported for chemotherapy-free immunotherapy in this setting and was achieved with only three cycles of treatment, supporting the feasibility of chemotherapy-free neoadjuvant approaches in patients who cannot or will not receive cisplatin.

The pCR rate of 8% in the nivolumab plus placebo group is lower than might have been expected. In PrE0807[24], neoadjuvant nivolumab monotherapy in 12 evaluable patients with cisplatin-ineligible cT2–T4a MIBC produced a pCR rate of 17% and an MPR rate of 25%, close to the 8% pCR and 23% MPR observed by local review, and very similar to the 17% pCR and 33% MPR observed by central review, in the nivolumab plus placebo control group of GDFATHER-NEO. The available data therefore do not provide strong evidence that the control group substantially underperformed; however, the possibility cannot be excluded given the small sample size. Because GDF-15 neutralization is expected to act on a mechanism of resistance that is not specific to a particular PD-1 or PD-L1 backbone, the combination of visugromab with more active regimens (for example, EVP) and other checkpoint inhibitors might yield higher efficacy and warrants formal evaluation.

Multiplex immunofluorescence identified a response-associated immune phenotype in the combination group, characterized by higher baseline densities of total $CD8^+$ and proliferating $CD8^+Ki\text{-}67^+$ T cells (Fig. 4b). Responses occurred across the range of centrally assessed PD-L1 CPS values, suggesting that PD-L1 CPS alone may be insufficient to identify responders. Baseline densities of total T cells, $CD8^+$ T cells and $CD8^+Ki\text{-}67^+$ T cells were numerically higher in group B, but between-group differences were not significant, the distributions overlapped substantially and the proliferating fraction of $CD8^+$ T cells was comparable between groups (Fig. 4a). Restricting the comparison to the range of baseline $CD8^+$ T cell density common to both groups (≤300 cells mm^{-2}), pCR was observed in 4 of 11 patients in group B and 1 of 12 in group A (Fig. 4a), suggesting that the greater antitumor activity of the combination was not explained by baseline immune infiltration alone. These observations are compatible with a model in which GDF-15 constrains the activity of preexisting intratumoral $CD8^+$ T cells and in which GDF-15 neutralization enables a more effective antitumor response. The small sample size and the exploratory nature of these analyses mean that this interpretation remains hypothesis-generating.

Neither circulating GDF-15 nor intratumoral pro-GDF-15 levels were associated with pathologic response or immune-cell infiltration. These findings contrast with previous reports that linked elevated baseline circulating GDF-15 concentrations to inferior outcomes for PD-1/PD-L1 blockade, as observed in metastatic melanoma[16] and advanced NSCLC[25]. They also differ in part from observations made in the GDFATHER-01, first-in-human phase 1/2 trial, where higher baseline serum and intratumoral GDF-15 levels were associated with reduced $CD8^+$ T cell infiltration and where GDF-15 blockade induced circulating CXCL9 and CXCL10[18]. Notably, median baseline circulating GDF-15 concentrations and intratumoral pro-GDF-15 abundance in GDFATHER-NEO were substantially lower than those reported in the metastatic melanoma and advanced NSCLC cohorts of GDFATHER-01. Cross-trial comparisons should therefore be interpreted with caution in light of given differences in GDF-15 abundance, disease type/setting, treatment duration difference, baseline immune composition and patient status (treatment naive versus advanced, relapsed/refractory). The pharmacodynamic significance of GDF-15-related biomarkers may therefore be context dependent and heavily impacted by the factors described above.

Given the association of clinical response to combination treatment in GDFATHER-NEO with baseline infiltration of $CD8^+$ T cells and proliferating $CD8^+$ T cells, functional immune states may be more informative specifically in early-stage disease with short-term treatment than static measurements of PD-L1 or GDF-15. However, this association requires further investigation and validation in independent cohorts to define the specific cellular programs involved and establish how GDF-15 reshapes the tumor immune microenvironment and influences responses to PD-1 blockade. The high pCR rate in the combination arm limited the availability of tumor-containing on-treatment biopsies, precluding a robust assessment of the intratumoral effects of GDF-15 blockade. Further translational studies will be needed to define how GDF-15 shapes antitumor immunity across disease settings and to identify biomarkers that most accurately capture biologically relevant GDF-15 activity.

The combination of nivolumab and visugromab was well tolerated, and the pattern of AEs was broadly similar in the two groups. No treatment-related deaths occurred, no patient discontinued the nivolumab plus visugromab combination because of toxicity—as opposed to two patients in the nivolumab control arm—and no delay for surgery or postoperative complication was attributed to neoadjuvant treatment (Table 2). No safety signal specific to visugromab emerged.

This exploratory trial has important limitations. With just 15 and 16 patients allocated per group, all estimates and the comparisons between groups are descriptive rather than inferential, despite a balanced distribution of key patient and tumor characteristics through participant stratification. Treatment was allocated sequentially within strata rather than by randomization[26]; sequential allocation does not provide concealment on the sponsor side and leaves the comparison susceptible to selection and period effects, although patients were blinded to treatment received. The allocation sequence was generated and applied centrally and was not disclosed to investigators, so that the next assignment within a stratum could not be anticipated at the time of enrollment. Once a patient had been allocated, investigators and sponsor staff were aware of the assigned treatment; patients were not. Formal randomization would, in addition, have protected against imbalance in unobserved confounders. Local and central pathologic review and central imaging review were performed in a blinded fashion. Finally, the small number of patients within each stratum limits the interpretation of the subgroup analyses, the exploratory biomarker analyses were not adjusted for multiple comparisons and the trial was conducted at only four centers in a single country.

In previously reported neoadjuvant series, pathologic nodal involvement has been uncommon or absent[27,28] among patients achieving ypT<2 disease, and given the exploratory nature of the trial, the protocol predefined reporting of ypT0 responses from radical

cystectomy and re-TURBT together. We note that one patient in group B who underwent re-TURBT (showing remaining local disease) followed by radical cystectomy was found to have N1 disease and was classified as a nonresponder, which illustrates the residual uncertainty attached to nodal status in patients not undergoing lymph node dissection. We recognize that this complicates comparison with other neoadjuvant trials in MIBC, but decided not to insist on RC and organ loss for endpoint assessment purposes. Patient reluctance to undergo cystectomy has increasingly affected recent neoadjuvant trials, reflecting both the greater efficacy of contemporary neoadjuvant regimens, with a larger proportion of patients achieving a complete response, and advances in staging, in the quality of transurethral resection and in the tolerability of these regimens relative to platinum-based chemotherapy. Together, these developments have made patients more willing to consider bladder preservation, even though the long-term oncologic safety of that approach has not been established.

Accounting for these limitations, the 33% pCR rate (47% in the central assessment) obtained with nivolumab plus visugromab is promising and within the range of the pCR (that is ypT0) proportions reported by the plethora of most active neoadjuvant studies using ICIs[6]. Radiographic and pathologic assessments were directionally concordant, but the agreement was imperfect: the centrally assessed radiographic complete response rate (13%) was considerably lower than the centrally assessed pCR rate (47%) in the combination group, whereas local assessment produced the opposite relationship. Imaging response alone therefore cannot be regarded as a surrogate for pathologic response in this setting, and its performance is likely to depend on center experience and on the imaging modality used.

Additional limitations include the relatively short duration of follow-up and the use of a protocol-defined efficacy-evaluable population for assessment of the pCR endpoint, both of which should be considered when interpreting the results and comparing them with other neoadjuvant MIBC trials.

In summary, the GDFATHER-NEO trial provides the first evidence that combined GDF-15 and PD-1 blockade may potentiate anti-PD-1 activity substantially in patients with previously untreated, checkpoint inhibitor-naive cancer, here in neoadjuvant treatment of MIBC. The combination with a Q4W schedule appears feasible and well tolerated. This tolerability may allow further combination into existing first-line immunotherapy schemes such as enfortumab vedotin plus pembrolizumab in neoadjuvant treatment of MIBC and treatment of advanced/metastatic urothelial cancer. Randomized phase 2b trials of visugromab are recruiting in treatment-naive advanced disease (NSCLC, NCT07098988) and in checkpoint inhibitor-refractory disease (NSCLC, NCT07246863 and hepatocellular carcinoma, NCT07219459) and will further inform on the ultimate clinical significance of GDF-15 blockade in these settings. Larger randomized trials in the neoadjuvant setting with long-term follow-up should be able to establish whether GDF-15 neutralization can improve bladder preservation, cure rates and overall survival in localized, immunoresponsive tumors such as MIBC.

Online content

Any methods, additional references, Nature Portfolio reporting summaries, source data, extended data, supplementary information, acknowledgements, peer review information; details of author contributions and competing interests; and statements of data and code availability are available at https://doi.org/10.1038/s41591-026-04740-9.

References

1. Filho, A. M., Briganti, A., Jemal, A. & Bray, F. Bladder cancer incidence and mortality: a global overview and recent trends. *Eur. Urol.* **89**, 426–436 (2026).
2. Powles, T. et al. ESMO Guidelines Committee. Bladder cancer: ESMO clinical practice guideline for diagnosis, treatment and follow-up. *Ann. Oncol.* **33**, 244–258 (2022).
3. Galsky, M. D., Ballas, L. & Kamat, A. M. Muscle-invasive bladder cancer: a watershed moment. *J. Clin. Oncol.* **43**, 3041–3051 (2025).
4. Powles, T. et al. Clinical efficacy and biomarker analysis of neoadjuvant atezolizumab in operable urothelial carcinoma in the ABACUS trial. *Nat. Med.* **25**, 1706–1714 (2019).
5. Necchi, A. et al. Updated results of PURE-01 with preliminary activity of neoadjuvant pembrolizumab in patients with muscle-invasive bladder carcinoma with variant histologies. *Eur. Urol.* **77**, 439–446 (2020).
6. Necchi, A. et al. Immunotherapy in the treatment of localized genitourinary cancers. *JAMA Oncol* **9**, 1447–1454 (2023).
7. Powles, T. et al. Perioperative durvalumab with neoadjuvant chemotherapy in operable bladder cancer. *N. Engl. J. Med.* **391**, 1773–1786 (2024).
8. Galsky, M. D. et al. Enfortumab vedotin and pembrolizumab in cisplatin-eligible bladder cancer. *N. Engl. J. Med.* **395**, 338–348 (2026).
9. Vulsteke, C. et al. Perioperative enfortumab vedotin and pembrolizumab in bladder cancer. *N. Engl. J. Med.* **394**, 1257–1269 (2026).
10. Powles, T. et al. ctDNA-guided adjuvant atezolizumab in muscle-invasive bladder cancer. *N. Engl. J. Med.* **393**, 2395–2408 (2025).
11. Necchi, A. et al. Gemcitabine intravesical system plus cetrelimab or cetrelimab alone as neoadjuvant therapy in muscle-invasive bladder cancer: SunRISe-4 primary analysis and biomarker results. *J. Clin. Oncol.* **44**, 586–597 (2026).
12. Awada, G. et al. The rapidly evolving paradigm of neoadjuvant immunotherapy across cancer types. *Nat. Cancer* **6**, 967–987 (2025).
13. Suartz, C. V. et al. Neoadjuvant immunotherapy in bladder cancer: ushering in a new era of treatment—a systematic review of current evidence. *Eur. Urol. Open Sci.* **79**, 45–59 (2025).
14. Chang, E. et al. Refining neoadjuvant therapy clinical trial design for muscle-invasive bladder cancer before cystectomy: a joint US Food and Drug Administration and Bladder Cancer Advocacy Network workshop. *Nat. Rev. Urol.* **19**, 37–46 (2022).
15. van Dijk, N. et al. Preoperative ipilimumab plus nivolumab in locoregionally advanced urothelial cancer: the NABUCCO trial. *Nat. Med.* **26**, 1839–1844 (2020).
16. Haake, M. et al. Tumor-derived GDF-15 blocks LFA-1 dependent T cell recruitment and suppresses responses to anti-PD-1 treatment. *Nat. Commun.* **14**, 4253 (2023).
17. Melero, I., Klar, K. & Leo, E. GDF-15 blockade: a multi-directional approach to potentiate cancer immunotherapy and alleviate cancer cachexia. *Clin. Transl. Med.* **15**, e70280 (2025).
18. Melero, I. et al. Neutralizing GDF-15 can overcome anti-PD-1 and anti-PD-L1 resistance in solid tumours. *Nature* **637**, 1218–1227 (2025).
19. Melero, I. et al. Long-term follow-up of a phase 1/2 trial of anti-GDF-15 antibody visugromab plus anti-PD-1 antibody nivolumab in anti-PD-1/-L1 relapsed/refractory solid tumors. *J. Hematol. Oncol.* **19**, 64 (2026).
20. Wischhusen, J., Melero, I. & Fridman, W. H. Growth/differentiation factor-15 (GDF-15): from biomarker to novel targetable immune checkpoint. *Front. Immunol.* **11**, 951 (2020).
21. Molina-Cerrillo, J. et al. Revisiting neoadjuvant chemotherapy in cisplatin-eligible muscle-invasive bladder cancer. *Eur. Urol. Oncol.* **9**, 168–180 (2026).
22. Blanc, J. et al. Avelumab-based neoadjuvant therapy in patients with muscle-invasive bladder cancer (AURA Oncodistinct-004): a phase 2 multicenter clinical trial. *J. Immunother. Cancer.* **13**, e012045 (2025).

23. Grande, E. et al. DUTRENEO trial: a randomized phase II trial of DUrvalumab and TREmelimumab versus chemotherapy as a NEOadjuvant approach to muscle-invasive urothelial bladder cancer (MIBC) patients (pts) prospectively selected by an interferon (INF)-gamma immune signature. *J. Clin. Oncol.* **38**, 5012 (2020).
24. Grivas, P. et al. PrECOG PrE0807: a phase 1b feasibility trial of neoadjuvant nivolumab without and with lirilumab in patients with muscle-invasive bladder cancer ineligible for or refusing cisplatin-based neoadjuvant chemotherapy. *Eur. Urol. Oncol.* **7**, 914–922 (2024).
25. Hong, G. et al. Plasma GDF15 levels associated with circulating immune cells predict the efficacy of PD-1/PD-L1 inhibitor treatment and prognosis in patients with advanced non-small cell lung cancer. *J. Cancer Res. Clin. Oncol.* **149**, 159–171 (2023).
26. Schulz, K. F. et al. 'Allocation concealment': the evolution and adoption of a methodological term. *J. R. Soc. Med.* **111**, 216–224 (2018).
27. Necchi, A. et al. Pembrolizumab as Neoadjuvant Therapy Before Radical Cystectomy in Patients with Muscle-Invasive Urothelial Bladder Carcinoma (PURE-01): an open-label, single-arm, phase II study. *J. Clin. Oncol.* **36**, 3353–3360 (2018).
28. Mercinelli, C. et al. First results of NURE-combo: a phase II study of neoadjuvant nivolumab and nab-paclitaxel, followed by postsurgical adjuvant nivolumab, for muscle-invasive bladder cancer. *J. Clin. Oncol.* **42**, 4196–4205 (2024).

Publisher's note Springer Nature remains neutral with regard to jurisdictional claims in published maps and institutional affiliations.

Open Access This article is licensed under a Creative Commons Attribution-NonCommercial-NoDerivatives 4.0 International License, which permits any non-commercial use, sharing, distribution and reproduction in any medium or format, as long as you give appropriate credit to the original author(s) and the source, provide a link to the Creative Commons licence, and indicate if you modified the licensed material. You do not have permission under this licence to share adapted material derived from this article or parts of it. The images or other third party material in this article are included in the article's Creative Commons licence, unless indicated otherwise in a credit line to the material. If material is not included in the article's Creative Commons licence and your intended use is not permitted by statutory regulation or exceeds the permitted use, you will need to obtain permission directly from the copyright holder. To view a copy of this licence, visit http://creativecommons.org/licenses/by-nc-nd/4.0/.

© The Author(s) 2026

Andrea Necchi[1,2] ✉, Chiara Mercinelli[1,2], Brigida A. Maiorano[1], Michela Piacentini[1], Antonio Cigliola[1,2], Roberto Iacovelli[3,4], Chiara Ciccarese[3,4], Chiara Ligato[3,4], Patrizia Giannatempo[5], Alessandro Rametta[5], Paolo Gontero[6,7], Francesco Soria[6], Christine Schuberth-Wagner[8], Joerg Wischhusen[9], Bernhard Rössler[8], Michael Metterlein[8], Stefan Ries[8], Thorsten Ross[8], Aasim Amin[8], Tobias Dreker[8], Frank Hermann[8], Lena Lemke[8], Kathrin Klar[8], Olga Mitina[8], Ana Kamova[8], Petra Fettes[8], Alexandra Auckenthaler[8], Sujata Rao[8], Eugen Leo[8,10] & Felix S. Lichtenegger[8,10]

[1]Department of Medical Oncology, IRCCS San Raffaele Hospital, Comprehensive Cancer Center, Milan, Italy. [2]Vita-Salute San Raffaele University, Milan, Italy. [3]Department of Oncology, Fondazione Policlinico Universitario Agostino Gemelli, Rome, Italy. [4]Translational Medicine and Surgery, Università Cattolica del Sacro Cuore, Rome, Italy. [5]Department of Medical Oncology, Fondazione IRCCS Istituto Nazionale dei Tumori, Milan, Italy. [6]Division of Urology, Department of Surgical Sciences, San Giovanni Battista Hospital, Turin, Italy. [7]University of Turin, Turin, Italy. [8]CatalYm GmbH, Munich, Germany. [9]Department of Gynecology, University Hospital Würzburg, Würzburg, Germany. [10]These authors jointly supervised this work: Eugen Leo, Felix S. Lichtenegger. ✉e-mail: necchi.andrea@hsr.it

Methods

Trial design and oversight

GDFATHER-NEO (NCT06059547; EudraCT 2022-002816-22; EU CT 2024-513957-55-00) is an exploratory, stratified, participant-blinded, parallel-group phase 2a trial of neoadjuvant PD-1 blockade with or without GDF-15 neutralization in patients with MIBC who are ineligible for or who decline cisplatin-based chemotherapy. Before allocation, patients were stratified by clinical tumor stage (T2 versus T3–T4a) and by PD-L1 expression on tumor and immune cells, determined by local pathology as a combined positive score (CPS ≥10 versus <10), into one of four strata: T2 and CPS <10, T2 and CPS ≥10, T3–T4a and CPS <10, and T3–T4a and CPS ≥10 (Fig. 1b).

Within each stratum, patients were allocated 1:1 to nivolumab plus visugromab (group B) or to nivolumab plus placebo (group A). Allocation was performed centrally and sequentially within each stratum (A–B–A–B, …) until at least 12 efficacy-evaluable patients had been allocated to each group. Sequential allocation with blinding of patients, rather than randomization, was chosen because of the small size of the individual strata, to prevent imbalance between treatment arms, and because this was the first evaluation of combined GDF-15 and PD-1 blockade in patients with early-stage disease treated with curative intent. Investigators and sponsor staff were aware of treatment allocation; patients were not. Local pathologists and the independent central pathology and imaging reviewers assessed responses without knowledge of treatment allocation.

The trial was sponsored by CatalYm GmbH (Munich, Germany). The protocol and its amendments were approved by the competent ethics committee of the coordinating center (Comitato Etico Territoriale Lombardia 1) and by the Italian regulatory authority (Agencia Italiana del Farmaco), and the trial was conducted in accordance with the principles of the Declaration of Helsinki, the guidelines for Good Clinical Practice of the International Council for Harmonisation and applicable local law. All patients provided written informed consent before any trial-specific procedure and received no compensation for participation.

The clinical cutoff date was 15 July 2026 for the analyses reported here and was supplemented by central review, bioanalytical and translational data. Data management, biometrics, on-site monitoring and bioanalytical and translational analyses were performed by, or under the oversight of, the sponsor. Independent central review of surgical specimens (pathologic response) and of imaging (radiographic response) was performed by Discovery Life Sciences Biomarker Services GmbH and by Median Technologies, respectively.

Participants

Patients aged ≥18 years with newly diagnosed cT2–T4a N0 M0 MIBC who were ineligible for cisplatin-based chemotherapy according to the modified Galsky criteria[29] or who declined such therapy, and who were considered fit to undergo radical cystectomy after 12 weeks of neoadjuvant therapy, were eligible. Clinical staging by CT was mandatory; positron emission tomography (PET)–CT and multiparametric MRI (mpMRI) were optional. Archival tumor material from a TURBT performed within 3 months before the start of treatment had to be available as a paraffin block. Only patients with an Eastern Cooperative Oncology Group performance status of 0 or 1 were eligible.

Further inclusion criteria were adequate bone marrow function (haemoglobin ≥10 g dl^{-1}, platelet count ≥100 × 10^9 l^{-1}, leukocyte count ≥2.5 × 10^9 l^{-1}), adequate hepatic function (aspartate and alanine aminotransferase ≤2× the upper limit of normal (ULN); bilirubin ≤1.5 × ULN), adequate renal function (serum creatinine <1.5× ULN and/or creatinine clearance ≥50 ml min^{-1}) and coagulation parameters within the normal range. Patients with type 2 diabetes mellitus had to discontinue metformin, which alters circulating GDF-15 concentrations, and switch to an alternative antidiabetic agent before the start of treatment.

Patients who had received prior systemic anticancer therapy, prior radiotherapy to the bladder tumor or a partial cystectomy, and patients who declined radical cystectomy at the time of trial entry were excluded. Patients with major tissue injury, clinically significant cardiovascular disease, active autoimmune disease, chronic high-dose systemic corticosteroid treatment or known or expected hypersensitivity to visugromab or nivolumab were also excluded. Full eligibility criteria are provided in the trial protocol (Supplementary Information). Sex was recorded as documented in the medical record and was used for descriptive purposes only; because of the small sample size, no sex- or gender-based analyses were prespecified, and none were performed.

Surgical procedures

A TURBT performed according to local practice within 3 months before the start of treatment was required for every patient, for histological characterization and staging. The resulting paraffin-embedded tumor material had to be made available for the additional histological and molecular analyses of the trial, in particular for PD-L1 CPS scoring; residual material was returned to the providing pathology department on request.

The trial comprised a screening phase of up to 4 weeks, beginning on the day written informed consent was obtained, and a core phase of 19 weeks, beginning on the day of the first administration of trial treatment. The core phase comprised the three 4-week immunotherapy cycles and a window of 4–8 weeks after the last neoadjuvant dose during which surgery was to be performed. Radical cystectomy or re-TURBT was planned at the time of trial entry and provided the surgical specimen (paraffin block) required for the assessment of pathologic response.

After completion of neoadjuvant treatment, and at the discretion of the investigator and the patient, one of the following procedures was performed, in line with the recommendations of the European Association of Urology: RC with pelvic lymph node dissection (PLND); or maximal re-TURBT, with adjuvant chemoradiotherapy or adjuvant nivolumab to be considered as clinically appropriate.

Provision of tumor material for the assessment of pathologic response and of immune cell infiltration was mandatory irrespective of whether a radical or a bladder-sparing approach was chosen. Surgical procedures followed each center's standard practice. Patients who declined, or who were unsuitable for, RC or re-TURBT after neoadjuvant treatment were managed according to European Association of Urology guidelines, which recommend chemoradiotherapy as the principal organ-sparing option. An end-of-treatment (EoT) visit was scheduled 21 days (±2 days) after completion of the surgical procedure.

Neoadjuvant treatment and procedures

Visugromab (CTL-002) is an investigational, humanized, hinge-stabilized immunoglobulin G4 (IgG4) monoclonal antibody that binds GDF-15 with high affinity. It was administered intravenously over approximately 60 min every 4 weeks (Q4W) at 20 mg kg^{-1}. Pharmacokinetic–pharmacodynamic modeling of data from the first-in-human trial indicated that, in combination with nivolumab, complete neutralization of circulating GDF-15 is achieved with 10 mg kg^{-1} every 2 weeks or with 20 mg kg^{-1} every 3–4 weeks.

Nivolumab, a fully human IgG4 monoclonal antibody directed against PD-1, was administered in accordance with its summary of product characteristics[30] and local guidelines. The 480 mg Q4W schedule was selected so that both agents could be given on the same 4-weekly visit schedule (Fig. 1b).

In group B, nivolumab and visugromab were given on day 1 of each of the three cycles, with visugromab administered first, and followed by a 30-min observation period before the nivolumab infusion. In group A, patients received placebo (drug-free infusion bags identical in appearance to the visugromab bags) before nivolumab, on the same schedule.

AEs were graded according to the National Cancer Institute Common Terminology Criteria for Adverse Events version 5.0[31] and were managed according to toxicity-specific algorithms defined in the protocol. Guidance on optional premedication before visugromab and on dose interruption of nivolumab and visugromab in the event of immune-related AEs was provided to investigators in the protocol (Supplementary Information).

Clinical assessments and outcomes

The primary objective was to assess the antitumor activity of visugromab in combination with nivolumab. Secondary objectives were to assess the safety and tolerability of the combination, its pharmacokinetics and pharmacodynamics, the development of antidrug antibodies (ADAs), and clinical outcomes in the neoadjuvant setting. Collection of molecular and genomic profiling data from peripheral blood and tumor tissue was an exploratory objective. Optional ^{18}F-fluorodeoxyglucose PET–CT and mpMRI were permitted for exploratory response assessment.

The two primary endpoints were the rate of pCR, determined by blinded local pathologists, and the rate of radiographic response according to RECIST version 1.1[32], determined by investigators. Secondary endpoints were AEs and serious AEs (SAEs), ADAs, delay of surgery, the rate of major pathologic response (MPR), event-free survival (EFS), time to relapse and overall survival (OS), standard pharmacokinetic parameters, baseline serum GDF-15 concentrations, and pCR, MPR and radiographic response as determined by independent central review.

pCR was defined as the absence of any residual viable tumor in the RC or re-TURBT specimen. Where a re-TURBT was followed by an RC, the pathologic evaluation of the RC specimen was used. Residual non-muscle-invasive disease (ypTa or ypT1) and residual carcinoma in situ were not considered a pCR. MPR was defined as ypT0/Ta/Tis/T1 N0 M0 after RC or ypT0/Ta/Tis/T1 NX M0 after re-TURBT, and therefore includes pCR. Radiographic response rate was defined as the proportion of patients with a complete or partial response according to RECIST version 1.1. Four protocol amendments took place. One implemented clarifications requested by local authorities (Italy) before the start of patient enrolment (removal of need for mandatory hospitalization after first administration of study medication in cycle 1 and extension of screening period to 28 days). A second amendment introduced re-TURBT as a surgical alternative to RC together with the assessment of ADAs as an additional secondary endpoint. A third amendment allowed inclusion of participants with stable atrial fibrillation. Post-enrollment, by the fourth amendment, central pathological review (for pCR) and central radiographic review (for ORR) were formally established as secondary endpoints (complementary central review had been mentioned in early protocol versions already) in line with clarifications on definitions of pCR and MPR.

A safety follow-up visit was scheduled 90 days (±3 days) after the last neoadjuvant dose to capture all AEs and SAEs occurring after neoadjuvant treatment, including postoperative complications. Longer-term outcomes were captured at follow-up visits for up to 12 months after RC or re-TURBT.

Exploratory biomarker endpoints, serum visugromab and ADA measurements

For the assessment of total visugromab, serum samples were collected 30 min before infusion and immediately before the end of infusion during cycles 1–3, on days 2 and 8 of cycle 1 and at the EoT visit. For the assessment of ADAs, serum samples were collected 30 min before infusion on day 1 of cycles 1–3 and at the EoT visit. Serum was isolated using standard procedures, cryopreserved at −80°C and analyzed using validated electrochemiluminescence assays for total visugromab and for ADA detection.

Formalin-fixed, paraffin-embedded (FFPE) tumor tissue obtained at screening (TURBT) and at post-treatment RC or re-TURBT was sectioned at 4 µm. After histological confirmation of tumor content on H&E-stained sections, multiplex immunofluorescence was performed using a validated 6 + 1-plex OPAL assay (Akoya Biosciences) on a Leica Bond Rx automated staining platform (BOND-RX software version 7.0.3.216, Leica Biosystems). The panel comprised CD4 (F7.2.38, Cell Marque), CD8 (C8/144B, Agilent), Ki-67 (MIB-1, Agilent), FoxP3 (SP97, Abcam), PD-L1 (SP263, Roche) and GDF-15 (HPA011191, Sigma-Aldrich). Chromogenic immunohistochemistry for pan-cytokeratin (AE1/AE3, Agilent) was subsequently performed on the same slide using a Ventana Discovery Ultra platform (software version 12.5 or higher) to enable segmentation of tumor compartments.

Whole-slide multispectral fluorescence imaging was performed at 20× magnification using an Akoya PhenoImager HT/Vectra Polaris platform (software version 1.0.13), followed by bright-field scanning after pan-cytokeratin staining. Pathologist-assisted digital image analysis was performed using validated Visiopharm algorithms (version 2021.09.2.11085, Visiopharm). Tumor, stromal and adjacent non-neoplastic tissue compartments were segmented on the basis of pan-cytokeratin staining, and predefined immune cell and biomarker-positive populations were quantified as cell densities (cells mm^{-2}) and as relative proportions within each compartment. Staining quality was assessed using on-slide and internal tissue controls, and markers that failed predefined quality criteria were excluded from downstream analyses.

Visiopharm assigns each detected cell to a single, mutually exclusive phenotype; cells co-expressing several markers (for example, CD8$^+$Ki-67$^+$) are therefore not included in the corresponding single-positive populations. To derive total marker-positive cell densities, composite variables were reconstructed by summing all mutually exclusive phenotypes containing the marker of interest. All reconstructed densities were calculated within the same tissue compartment and are expressed as cells per square millimeter.

All assays were performed according to predefined analytical procedures and validation criteria established for exploratory profiling of the tumor microenvironment and of GDF-15 biology.

Evaluation of intratumoral pro-GDF-15 expression in human FFPE samples

Intratumoral pro-GDF-15 expression was determined using a rabbit polyclonal anti-GDF-15 antibody (HPA011191, Sigma-Aldrich) as the primary antibody, with automated staining on a Ventana BenchMark Ultra platform (Roche; software versions 12.3.1 and 12.5.4). Binding of the anti-GDF-15 antibody was visualized using a secondary horseradish peroxidase-conjugated antibody (Ventana OptiView Universal DAB Detection Kit, 760-700; Roche Diagnostics) and a precipitating enzyme reaction product. Slides were evaluated by a board-certified pathologist who scored cytoplasmic staining of tumor cells and, where applicable, membranous staining. Cytoplasmic staining was assigned to four intensity categories, from 0 (no staining) to 3+ (intense staining), and the percentage of stained cells in each category was recorded. The H score, which reflects tumor GDF-15 protein levels, was calculated by summing the products of the percentage of cells in each category and the corresponding intensity value, as follows:

$$\begin{aligned}\text{H score} = {} & [1 \times (\text{percentage of intensity1})] \\ & + [2 \times (\text{percentage of intensity2})] \\ & + [3 \times (\text{percentage of intensity3})]\end{aligned}$$

Central evaluation of PD-L1 protein expression in human FFPE samples

PD-L1 expression was assessed centrally by immunohistochemistry using the SP263 assay (790-4905; Roche Diagnostics) according to the manufacturer's protocol, with a rabbit IgG monoclonal antibody (790-4795; Roche Diagnostics) as isotype control. Staining was evaluated by

a board-certified pathologist, and the tumor proportion score (TPS) and CPS were determined as previously described.

Measurement of cytokine and chemokine levels in patient samples

Serum samples for cytokine and chemokine analysis were collected 30 min before infusion on day 1 of cycles 1–3 and at the EoT visit. CXCL9 (MIG) and CXCL10 (IP-10) concentrations were measured using validated ELISAs (Human CXCL9/MIG Quantikine ELISA Kit, DCX900; Human CXCL10/IP-10 Quantikine ELISA Kit, DIP100; R&D Systems). IFN-γ concentrations were determined using a validated multiplex immunoassay (V-PLEX Plus Proinflammatory Panel 1 (human) Kit, K15049G; Meso Scale Discovery). For graphical presentation and statistical analysis, concentrations below the LLOQ were assigned a value of LLOQ/2. All assays were performed in compliance with Good Laboratory Practice.

Statistical analysis

This exploratory, stratified, participant-blinded, parallel-group phase 2a trial was descriptive in design. No formal sample size calculation was performed, and no hypothesis was tested; the trial was not powered to detect a difference between treatment groups, and all comparisons between groups are exploratory. Continuous variables are summarized by number of observations, mean, median, minimum and maximum; categorical variables are summarized by counts and percentages. Percentages are calculated using the number of evaluable patients in the relevant analysis population as the denominator. Presented confidence intervals are 95% exact binomial (Clopper–Pearson) confidence intervals.

The safety analysis population comprised all patients who received at least one dose of trial treatment; it was identical to the intention-to-treat population. Safety data are summarized by treatment group and visit. The efficacy analysis population comprised all patients who received at least one infusion and underwent RC or re-TURBT, unless surgery had been precluded by confirmed disease progression or by discontinuation for toxicity. Separate efficacy analysis populations were defined for locally and for centrally assessed pathologic and radiographic response, as detailed in Fig. 1a. In case of early discontinuation due to confirmed disease progression or toxicity, participants were considered as nonresponders for the primary and secondary endpoint analyses of histopathological and radiographic response.

Two-group comparisons of continuous variables were made using the two-sided Mann–Whitney *U* test. Because of the small sample sizes and the potentially nonnormal distributions of biomarker measurements, no assumption of normality was made, and comparisons were performed using this nonparametric test. No adjustment was made for multiple comparisons, and no covariates were included in the exploratory biomarker comparisons. Exact *P* values are reported in the corresponding figures and figure legends; values exceeding the software reporting limit are shown as $P > 0.9999$. All *P* values are reported descriptively, and no inferential claim is made, given the exploratory design and the small sample size. Analyses were performed using GraphPad Prism version 11.0.0 (GraphPad Software).

Time-to-event endpoints were summarized using the Kaplan–Meier method. Response rates are presented as the number and proportion of responders in each treatment group.

Reporting summary

Further information on research design is available in the Nature Portfolio Reporting Summary linked to this article.

Data availability

Individual participant data underlying this Article are held by the sponsor. In line with Regulation (EU) No. 536/2014 and with the requirements for transparent reporting of clinical trials in WHO primary registries, aggregated results will be posted to the trial registries and a full clinical trial report will be prepared. Additional source data files supporting the findings of this trial are provided as Supplementary Information. Requests for access to de-identified individual participant data may be submitted to the sponsor at info@catalym.com and will be reviewed on the basis of a methodologically sound proposal, subject to the terms of the informed consent obtained and to the General Data Protection Regulation; approved requests require a data access agreement. Source data are provided with this paper.

Code availability

No custom code or mathematical algorithm was specifically developed for this study. Software and packages used in the analyses can be found in the Methods or in the Reporting Summary.

References

29. Jiang, D. M. et al. Defining cisplatin eligibility in patients with muscle-invasive bladder cancer. *Nat. Rev. Urol.* **18**, 104–114 (2021).
30. Opdivo SmPC (marketing authorisation holder: Bristol-Myers Squibb Pharma EEIG). *European Medicines Agency* https://www.ema.europa.eu/en/medicines/human/EPAR/opdivo#product-info (2026).
31. US Department of Health and Human Services. Common Terminology Criteria for Adverse Events (CTCAE) v5.0. *U.S. National Cancer Institute, Division of Cancer Therapy and Diagnosis* https://ctep.cancer.gov/protocolDevelopment/electronic_applications/docs/CTCAE_v5_Quick_Reference_5x7.pdf (2017).
32. Eisenhauer, E. A. et al. New response evaluation criteria in solid tumours: revised RECIST guideline (version 1.1). *Eur. J. Cancer* **45**, 228–247 (2009).

Acknowledgements

The investigators thank the participants and the staff members at the trial sites who managed and cared for them; the members of the data monitoring committee; F. Montorsi and A. Briganti (both Milan) for contributing patients for this trial; G. Brambilla (Milan) for imaging response review; the staff of Precision for Medicine (Edinburgh, UK) and of Metronomia (Munich, Germany) involved in data collection and analyses; the staff of Discovery Life Sciences (Kassel, Germany) for performing the central histopathological assessment of the tumor tissue specimens; M. Foster, consultant pathologist, for expert histopathological review; and M. Hartmann from Ecc-Oncology (Trier, Germany) for medical writing. The funder of the trial provided nivolumab free of cost and provided third-party funding for trial coordination, documentation, monitoring and data management. Medical writing and editing support, funded by CatalYm GmbH, was provided by Markus Hartmann, PhD, European Consulting & Contracting in Oncology, Trier, Germany.

Author contributions

A.N., E.L., F.S.L., F.H. and J.W. conceptualized the trial. A.N., C.M., B.A.M., M.P., A.C., R.I., C.C., C.L., P. Giannatempo, A.R., P. Gontero., F.S., A. Amin, M.M., L.L., O.M., A.K., P.F., A. Auckenthaler and F.S.L. were responsible for data curation; A.N. had access to the clinical trial's raw data. T.R., K.K., A. Amin, T.D., L.L., O.M., A.K., P.F., A. Auckenthaler, S. Rao, E.L. and F.S.L. performed the formal analysis. A.N., C.M., B.A.M., M.P., A.C., R.I., C.C., C.L., P. Giannatempo, A.R., P. Gontero. and F.S. conducted the clinical investigations. E.L., F.S.L., F.H., T.R., K.K. and P.F. were responsible for the methodology. B.R., O.M., A.K., A. Auckenthaler and P.F. were responsible for project administration. E.L. and C.S.W. were responsible for funding acquisition. A.N., E.L., F.S.L., S. Rao, S. Ries, K.K. and P.F. supervised the project. A. Amin, T.D., L.L., K.K., T.R., E.L. and F.S.L. performed validations. T.R., K.K., A. Amin, T.D.,

L.L., O.M., A.K., E.L. and F.S.L. generated visualizations. All authors participated in the writing or critical review and editing of the paper. All authors approved the paper for submission for publication.

Funding

The trial was sponsored and funded by CatalYm GmbH (Munich, Germany), which financially supported all trial-related procedures and provided the investigational medicinal products. No specific trial-related grants supported this work except for J.W.

Competing interests

J.W. is a co-founder of the biotech company CatalYm GmbH, owner of GDF-15 related patents and stock owner of CatalYm GmbH. C.S.W., B.R., M.M., S. Ries, T.R., K.K., A. Amin, T.D., F.H., L.L., O.M., A.K., P.F., A. Auckenthaler, S. Rao., E.L. and F.S.L. are current or former employees of CatalYm GmbH and/or hold stock options of CatalYm GmbH. J.W. has received research funding or consulting and/or advisory fees from CatalYm GmbH. C.S.W., J.W., K.K., M.M., F.H. and E.L. are inventors on patents related to visugromab and anti-GDF-15 treatment. A.N., C.M., B.A.M., M.P., A.C., R.I., C.C., C.L., P. Giannatempo, A.R., P. Gontero and F.S. were clinical investigators; investigator fees were paid to their institutions. Several coauthors declare potentially competing interests (grants or contracts and/or royalties or licenses, stock or stock options, consulting fees, honoraria, travel or meeting support, or advisory or data safety monitoring board participation) apart from their relationship with CatalYm GmbH: A.N. (grants and consulting fees from AstraZeneca, Bristol-Myers Squibb, Merck Sharp & Dohme and Gilead Sciences; consulting fees from Johnson & Johnson, Samsung Bioepis, Daiichi Sankyo and Pfizer; meeting/travel support from Gilead, Johnson & Johnson and Merck Sharp & Dohme); C.M. (honoraria from Astellas and AstraZeneca; travel/meeting support from Bayer, Ipsen and Johnson & Johnson); B.A.M. (research funding from Merck Serono; consulting/advisory roles for Astellas, AstraZeneca, Bayer, Johnson & Johnson, Ipsen, Merck Serono and Merck Sharp & Dohme; meeting/travel support from Ipsen, Janssen, Novartis, Pfizer); A.C. (honoraria from Astellas and Merck Sharp & Dohme; meeting/travel support from Ipsen and Merck, Sharp & Dohme; advisory or safety monitoring board activities for Johnson & Johnson); R.I. (consulting fees and honoraria from Astellas, Bristol-Myers Squibb, Johnson & Johnson and Merck Sharp & Dohme; advisory or safety monitoring board activities for Astellas, Bristol-Myers Squibb, Johnson & Johnson, Merck Sharp & Dohme and Pfizer); C.C. (advisory board roles and/or meeting/travel support from Astellas, AstraZeneca, Bristol-Myers Squibb, Eisai, Ipsen, Janssen, Merck Sharp & Dohme, Novartis, Pfizer); P. Giannatempo (consulting fees, honoraria and travel/meeting support from Astellas, AstraZeneca, Johnson & Johnson, Merck and Merck Sharp & Dohme); P. Gontero (research grants and meeting/travel support from Intuitive Surgical and CRT Foundation; Consulting fees from AstraZeneca, Merck Sharp & Dohme, Pfizer and Photocure; honoraria from AstraZeneca, Ferring, Medac and Merck); F.S. (consulting fees from Accord, AstraZeneca, Cepheid, Ferring, Johnson & Johnson, Medac, Merck Sharp & Dohme, Pfizer and Photocure; honoraria from AstraZeneca, Johnson & Johnson and Medac; advisory or safety monitoring board activities for Accord, AstraZeneca, Cepheid, Ferring, Johnson & Johnson, Medac, Merck Sharp & Dohme and Pfizer); J.W. (research grants (Transcan-3) from the German Ministry for Education & Research; inventor royalties from patents owned by the Julius-Maximilians-University Würzburg); F.H. (consulting fees, co-ownership and stock options of Avenor Therapeutics; employment at Thermosome until March 2026); L.L. (stock options held from Novartis); and P.F. (stock options from Amgen and BioNTech). M.P., C.L. and A.R. declared no competing interests.

Additional information

Extended data is available for this paper at https://doi.org/10.1038/s41591-026-04740-9.

Supplementary information The online version contains supplementary material available at https://doi.org/10.1038/s41591-026-04740-9.

Correspondence and requests for materials should be addressed to Andrea Necchi.

Peer review information *Nature Medicine* thanks the anonymous reviewers for their contribution to the peer review of this work. Primary Handling Editor: Ulrike Harjes, in collaboration with the *Nature Medicine* team.

Reprints and permissions information is available at www.nature.com/reprints.

https://doi.org/10.1038/s41591-026-04740-9

Extended Data Table 1 | Allocation of patients to strata and treatment groups and assignment to primary endpoint analyses

Participant	Stratum (Cohort)	Treatment group	Number of cycles	Surgical intervention	Histopathol. Response (local)	Stage post-surgery (local)	Histopathol. Response (central)	Radiol. Response (local)	Radiol. Response (central)	Reason early termination	Status (15 Jul 2026)
#1	2	A (N+Pla)	C1 only	RC	pNR	pT3 N0	N/A	PD	SD	Discontinued early (AE)	Completed
#2	1	A (N+Pla)	C1-C3	Re-TURBT	pNR	pT2 Nx	pNR	SD	PD	--	Completed
#3	4	A (N+Pla)	C1-C3	RC	pNR	pT3 N1	pNR	SD	SD	--	Completed
#4	4	B (N+V)	C1-C3	not done	N/A	N/A	N/A	PR	SD	Withdrawal IC prior RC	Early termination *
#5	1	A (N+Pla)	C1-C3	RC	pNR	pT2 N0	MPR	PD	SD	--	Completed †
#6	3	A (N+Pla)	C1-C3	not done	N/A	N/A	N/A	N/A	N/A	Withdrawal IC prior RC	Early termination ‡
#7	1	B (N+V)	C1-C3	Re-TURBT	pCR	pT0 Nx	pCR	CR	PR	--	Completed
#8	2	B (N+V)	C1-C3	RC	MPR	TIS N0	pCR	CR	PR	--	Completed
#9	1	A (N+Pla)	C1-C3	Re-TURBT	MPR	pT1 Nx	MPR	SD	PR	--	Completed
#10	2	B (N+V)	C1-C3	RC	pCR	pT0 N0	pCR	CR	PR	--	Completed
#11	4	B (N+V)	C1-C3	RC	MPR	CIS N0	pCR	CR	SD	--	Completed
#12	2	B (N+V)	C1-C3	Re-TURBT	pCR	pT0 Nx	pCR	CR	PR	--	Completed
#13	2	A (N+Pla)	C1-C3	RC	MPR	pT1 N0	pCR	SD	PR	--	Completed
#14	2	A (N+Pla)	C1-C3	RC	pNR	pT3 N1	pNR	PD	SD	--	Completed
#15	1	B (N+V)	C1-C3	Re-TURBT→RC	pNR	pT0 N1	pNR	CR	CR	--	Completed
#16	4	B (N+V)	C1-C3	Re-TURBT	MPR	pT1 Nx	MPR	SD	PR	--	Completed
#17	2	B (N+V)	C1-C3	Re-TURBT	pCR	pT0 Nx	pCR	NE	SD	--	Completed
#18	1	B (N+V)	C1 only	RC	pNR	pT3 N1	pNR	PD	PD	Discontinued early (AE)	Completed
#19	4	B (N+V)	C1-C3	RC	MPR	pT1 N0	MPR	PR	PR	--	Completed
#20	1	B (N+V)	C1-C3	RC	pNR	pT2 Nx	pNR	SD	SD	--	Completed
#21	4	A (N+Pla)	C1-C3	RC	pNR	pT2 N0	pNR	SD	NE	--	Completed
#22	1	B (N+V)	C1-C3	RC	pNR	pT3 Nx	pNR	SD	PD	--	Completed
#23	3	B (N+V)	C1-C3	RC	pNR	pT4 N0	pNR	SD	SD	--	Completed
#24	3	B (N+V)	C1-C3	RC	pNR	pT3 N2	pNR	PD	SD	--	Completed
#25	4	A (N+Pla)	C1 only	not done¶	N/A¶	N/A¶	N/A¶	N/A¶	N/A¶	Discontinued early (AE)	Completed
#26	4	A (N+Pla)	C1-C3	RC	pNR	pT3 N0	pNR	SD	PD	--	Completed
#27	2	A (N+Pla)	C1-C3	RC	pNR	pT3 N2	pNR	SD	PD	--	Completed
#28	1	A (N+Pla)	C1-C3	RC	pNR	pT3 N0	pNR	SD	SD	--	Completed
#29	1	A (N+Pla)	C1-C3	RC	pCR	pT0 N0	pCR	PR	PR	--	Completed
#30	3	A (N+Pla)	C1-C3	Re-TURBT	pNR	pT2 Nx	MPR	PR	PR	--	Completed
#31	2	B (N+V)	C1-C3	Re-TURBT	pCR	pT0 Nx	pCR	CR	CR	--	Completed
n=31											

Abbreviations: C1–C3, treatment cycles 1 to 3 completed; CIS, carcinoma *in* situ; CR, complete response; MPR, major pathologic response; N, nivolumab; N/A, not available; NE, not evaluable; PD, progressive disease; Pla, placebo; pCR, pathologic complete response; pNR, no pathologic response; PR, partial response; RC, radical cystectomy; SD, stable disease; TURBT, transurethral resection of bladder tumor; V, visugromab. *No pathologic response assessment available, but evaluable for radiographic response. †Completed, but not included in evaluable population for pathologic or radiographic response due to misdosing. ‡No pathologic or radiographic response assessment available. ¶End-of-treatment visit performed early because of a serious adverse event; RC performed outside of trial, no result available; imputed non-responder for pathologic and radiographic assessment.

https://doi.org/10.1038/s41591-026-04740-9

Extended Data Table 2 | Any Adverse Events. System Organ Class / Preferred Term

	N+P (N=15) Patients n (%)		N+V (N=16) Patients n (%)		Total (N=31) Patients n (%)	
	Any Grade	Grade 3-4	Any Grade	Grade 3-4	Any Grade	Grade 3-4
Any Adverse Events	15 (100.0%)	12 (80.0%)	16 (100.0%)	8 (50.0%)	31 (100.0%)	20 (64.5%)
Renal and urinary disorders	8 (53.3%)	4 (26.7%)	6 (37.5%)	2 (12.5%)	14 (45.2%)	6 (19.4%)
Haematuria	4 (26.7%)	1 (6.7%)	2 (12.5%)	1 (6.2%)	6 (19.4%)	2 (6.5%)
Dysuria	3 (20.0%)	0 (0.0%)	0 (0.0%)	0 (0.0%)	3 (9.7%)	0 (0.0%)
Hydronephrosis	1 (6.7%)	1 (6.7%)	1 (6.2%)	1 (6.2%)	2 (6.5%)	2 (6.5%)
Oliguria	1 (6.7%)	1 (6.7%)	0 (0.0%)	0 (0.0%)	1 (3.2%)	1 (3.2%)
Pyelocaliectasis	1 (6.7%)	1 (6.7%)	0 (0.0%)	0 (0.0%)	1 (3.2%)	1 (3.2%)
Investigations	7 (46.7%)	2 (13.3%)	6 (37.5%)	1 (6.2%)	13 (41.9%)	3 (9.7%)
Alanine aminotransferase increased	3 (20.0%)	2 (13.3%)	2 (12.5%)	1 (6.2%)	5 (16.1%)	3 (9.7%)
Aspartate aminotransferase increased	2 (13.3%)	2 (13.3%)	2 (12.5%)	1 (6.2%)	4 (12.9%)	3 (9.7%)
General disorders and administration site conditions	6 (40.0%)	1 (6.7%)	7 (43.8%)	0 (0.0%)	13 (41.9%)	1 (3.2%)
Pyrexia	2 (13.3%)	1 (6.7%)	1 (6.2%)	0 (0.0%)	3 (9.7%)	1 (3.2%)
Blood and lymphatic system disorders	5 (33.3%)	1 (6.7%)	6 (37.5%)	0 (0.0%)	11 (35.5%)	1 (3.2%)
Anaemia	5 (33.3%)	1 (6.7%)	6 (37.5%)	0 (0.0%)	11 (35.5%)	1 (3.2%)
Infections and infestations	4 (26.7%)	4 (26.7%)	6 (37.5%)	3 (18.8%)	10 (32.3%)	7 (22.6%)
Urinary tract infection	2 (13.3%)	2 (13.3%)	1 (6.2%)	1 (6.2%)	3 (9.7%)	3 (9.7%)
Staphylococcal infection	0 (0.0%)	0 (0.0%)	2 (12.5%)	1 (6.2%)	2 (6.5%)	1 (3.2%)
Bacterial infection	0 (0.0%)	0 (0.0%)	1 (6.2%)	1 (6.2%)	1 (3.2%)	1 (3.2%)
Pneumonia	1 (6.7%)	1 (6.7%)	0 (0.0%)	0 (0.0%)	1 (3.2%)	1 (3.2%)
Sepsis	1 (6.7%)	1 (6.7%)	0 (0.0%)	0 (0.0%)	1 (3.2%)	1 (3.2%)
Urosepsis	1 (6.7%)	1 (6.7%)	0 (0.0%)	0 (0.0%)	1 (3.2%)	1 (3.2%)
Gastrointestinal disorders	4 (26.7%)	1 (6.7%)	4 (25.0%)	0 (0.0%)	8 (25.8%)	1 (3.2%)
Retroperitoneal hematoma	1 (6.7%)	1 (6.7%)	0 (0.0%)	0 (0.0%)	1 (3.2%)	1 (3.2%)
Metabolism and nutrition disorders	3 (20.0%)	2 (13.3%)	4 (25.0%)	0 (0.0%)	7 (22.6%)	2 (6.5%)
Hypokalaemia	2 (13.3%)	1 (6.7%)	0 (0.0%)	0 (0.0%)	2 (6.5%)	1 (3.2%)
Hyponatraemia	1 (6.7%)	1 (6.7%)	1 (6.2%)	0 (0.0%)	2 (6.5%)	1 (3.2%)
Musculoskeletal and connective tissue disorders	3 (20.0%)	1 (6.7%)	3 (18.8%)	0 (0.0%)	6 (19.4%)	1 (3.2%)
Myalgia	1 (6.7%)	1 (6.7%)	0 (0.0%)	0 (0.0%)	1 (3.2%)	1 (3.2%)
Endocrine disorders	2 (13.3%)	1 (6.7%)	4 (25.0%)	0 (0.0%)	6 (19.4%)	1 (3.2%)
Hypothyroidism	2 (13.3%)	1 (6.7%)	4 (25.0%)	0 (0.0%)	6 (19.4%)	1 (3.2%)
Vascular disorders	3 (20.0%)	2 (13.3%)	2 (12.5%)	1 (6.2%)	5 (16.1%)	3 (9.7%)
Hypertension	3 (20.0%)	2 (13.3%)	0 (0.0%)	0 (0.0%)	3 (9.7%)	2 (6.5%)
Lymphocele	0 (0.0%)	0 (0.0%)	1 (6.2%)	1 (6.2%)	1 (3.2%)	1 (3.2%)
Neoplasms benign, malignant and unspecified (incl. cysts and polyps)	2 (13.3%)	1 (6.7%)	3 (18.8%)	2 (12.5%)	5 (16.1%)	3 (9.7%)
Prostate cancer	1 (6.7%)	1 (6.7%)	3 (18.8%)	2 (12.5%)	4 (12.9%)	3 (9.7%)
Injury, poisoning and procedural complications	4 (26.7%)	3 (20.0%)	0 (0.0%)	0 (0.0%)	4 (12.9%)	3 (9.7%)
Fall	1 (6.7%)	1 (6.7%)	0 (0.0%)	0 (0.0%)	1 (3.2%)	1 (3.2%)
Seroma	1 (6.7%)	1 (6.7%)	0 (0.0%)	0 (0.0%)	1 (3.2%)	1 (3.2%)
Ureteric anastomosis complication	1 (6.7%)	1 (6.7%)	0 (0.0%)	0 (0.0%)	1 (3.2%)	1 (3.2%)
Vascular pseudoaneurysm	1 (6.7%)	1 (6.7%)	0 (0.0%)	0 (0.0%)	1 (3.2%)	1 (3.2%)
Cardiac disorders	2 (13.3%)	1 (6.7%)	2 (12.5%)	1 (6.2%)	4 (12.9%)	2 (6.5%)
Aortic valve stenosis	1 (6.7%)	1 (6.7%)	0 (0.0%)	0 (0.0%)	1 (3.2%)	1 (3.2%)
Atrial fibrillation	0 (0.0%)	0 (0.0%)	1 (6.2%)	1 (6.2%)	1 (3.2%)	1 (3.2%)
Respiratory, thoracic and mediastinal disorders	2 (13.3%)	0 (0.0%)	1 (6.2%)	1 (6.2%)	3 (9.7%)	1 (3.2%)
Interstitial lung disease	0 (0.0%)	0 (0.0%)	1 (6.2%)	1 (6.2%)	1 (3.2%)	1 (3.2%)
Hepatobiliary disorders	1 (6.7%)	0 (0.0%)	1 (6.2%)	1 (6.2%)	2 (6.5%)	1 (3.2%)

https://doi.org/10.1038/s41591-026-04740-9

Extended Data Table 2 (continued) | Any Adverse Events. System Organ Class / Preferred Term

	N+P (N=15) Patients n (%)		N+V (N=16) Patients n (%)		Total (N=31) Patients n (%)	
	Any Grade	**Grade 3-4**	**Any Grade**	**Grade 3-4**	**Any Grade**	**Grade 3-4**
Immune-mediated hepatic disorder	0 (0.0%)	0 (0.0%)	1 (6.2%)	1 (6.2%)	1 (3.2%)	1 (3.2%)
	Any grade		**Any grade**		**Any grade**	
Serious AE	7 (46.7%)		8 (50.0%)		15 (48.4%)	
Infections and infestations	2 (13.3%)		3 (18.8%)		5 (16.1%)	
Bacterial infection	0 (0.0%)		1 (6.2%)		1 (3.2%)	
Sepsis	1 (6.7%)		0 (0.0%)		1 (3.2%)	
Staphylococcal infection	0 (0.0%)		1 (6.2%)		1 (3.2%)	
Urinary tract infection	0 (0.0%)		1 (6.2%)		1 (3.2%)	
Urosepsis	1 (6.7%)		0 (0.0%)		1 (3.2%)	
Renal and urinary disorders	3 (20.0%)		1 (6.2%)		4 (12.9%)	
Haematuria	2 (13.3%)		0 (0.0%)		2 (6.5%)	
Hydronephrosis	1 (6.7%)		0 (0.0%)		1 (3.2%)	
Hydroureter	0 (0.0%)		1 (6.2%)		1 (3.2%)	
Oliguria	1 (6.7%)		0 (0.0%)		1 (3.2%)	
Neoplasms benign, malignant and unspecified (incl. cysts and polyps)	1 (6.7%)		3 (18.8%)		4 (12.9%)	
Prostate cancer	1 (6.7%)		3 (18.8%)		4 (12.9%)	
Metabolism and nutrition disorders	1 (6.7%)		1 (6.2%)		2 (6.5%)	
Hypercreatininaemia	0 (0.0%)		1 (6.2%)		1 (3.2%)	
Hyponatraemia	1 (6.7%)		0 (0.0%)		1 (3.2%)	
Injury, poisoning and procedural complications	2 (13.3%)		0 (0.0%)		2 (6.5%)	
Fall	1 (6.7%)		0 (0.0%)		1 (3.2%)	
Ureteric anastomosis complication	1 (6.7%)		0 (0.0%)		1 (3.2%)	
Vascular pseudoaneurysm	1 (6.7%)		0 (0.0%)		1 (3.2%)	
Cardiac disorders	1 (6.7%)		1 (6.2%)		2 (6.5%)	
Aortic valve stenosis	1 (6.7%)		0 (0.0%)		1(3.2%)	
Atrial fibrillation	0 (0.0%)		1 (6.2%)		1 (3.2%)	
Respiratory, thoracic and mediastinal disorders	0 (0.0%)		1 (6.2%)		1 (3.2%)	
Interstitial lung disease	0 (0.0%)		1 (6.2%)		1 (3.2%)	
Hepatobiliary disorders	0 (0.0%)		1 (6.2%)		1 (3.2%)	
Immune-mediated hepatic disorder	0 (0.0%)		1 (6.2%)		1 (3.2%)	
General disorders and administration site conditions	1 (6.7%)		0 (0.0%)		1 (3.2%)	
Pyrexia	1 (6.7%)		0 (0.0%)		1 (3.2%)	
Endocrine disorders	1 (6.7%)		0 (0.0%)		1 (3.2%)	
Hypothyroidism	1 (6.7%)		0 (0.0%)		1 (3.2%)	
	Any grade		Any grade		Any grade	
Immune-related adverse events	4 (26.7%)		5 (31.3%)		9 (29.0%)	
	Any grade		Any grade		Any grade	
AE leading to discontinuation	2 (13.3%)		0 (0%)		2 (6.5%)	
Investigations	1 (6.7%)		0 (0.0%)		1 (3.2%)	
Aspartate aminotransferase increased	1 (6.7%)		0 (0.0%)		1 (3.2%)	
Musculoskeletal and connective tissue disorders	1 (6.7%)		0 (0.0%)		1 (3.2%)	
Myalgia	1 (6.7%)		0 (0.0%)		1 (3.2%)	

Abbreviations: N+P, nivolumab plus placebo; N+V, nivolumab plus visugromab. Adverse events by MedDRA Preferred Term (PT). Terms in bold in the left column refer to System Organ Class (SOC) terms.

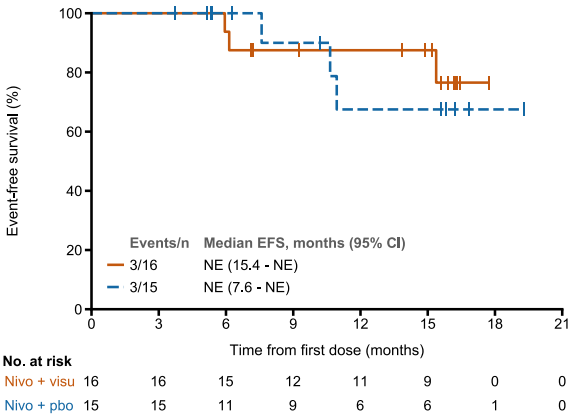
https://doi.org/10.1038/s41591-026-04740-9

Extended Data Table 3 | Any immune-related Adverse Events. System Organ Class / Preferred Term

	N+P (N=15) Patients n (%)		N+V (N=16) Patients n (%)		Total (N=31) Patients n (%)	
	Any Grade	**Grade 3-4**	**Any Grade**	**Grade 3-4**	**Any Grade**	**Grade 3-4**
Any immune related Adverse Events	4 (26.7%)	3 (20.0%)	5 (31.3%)	2 (12.5%)	9 (29.0%)	5 (16.1%)
Endocrine disorders	2 (13.3%)	1 (6.7%)	2 (12.5%)	0	4 (12.9%)	1 (3.2%)
Hypothyroidism	2 (13.3%)	1 (6.7%)	2 (12.5%)	0	4 (12.9%)	1 (3.2%)
Hyperthyroidism	1 (6.7%)	0	0	0	1 (3.2%)	0
Hepatobiliary disorders	1 (6.7%)	0	1 (6.2%)	1 (6.2%)	2 (6.5%)	1 (3.2%)
Hepatic steatosis	1 (6.7%)	0	0	0	1 (3.2%)	0
Immune-mediated hepatic disorder	0	0	1 (6.2%)	1 (6.2%)	1 (3.2%)	1 (3.2%)
Skin and subcutaneous tissue disorders	0	0	2 (12.5%)	0	2 (6.5%)	0
Lichen planus	0	0	1 (6.2%)	0	1 (3.2%)	0
Pruritus	0	0	1 (6.2%)	0	1 (3.2%)	0
Investigations	1 (6.7%)	1 (6.7%)	0	0	1 (3.2%)	1 (3.2%)
Alanine aminotransferase increased	1 (6.7%)	1 (6.7%)	0	0	1 (3.2%)	1 (3.2%)
Aspartate aminotransferase increased	1 (6.7%)	1 (6.7%)	0	0	1 (3.2%)	1 (3.2%)
Gamma-glutamyl transferase increased	1 (6.7%)	0	0	0	1 (3.2%)	0
Musculoskeletal and connective tissue disorders	1 (6.7%)	1 (6.7%)	0	0	1 (3.2%)	1 (3.2%)
Arthralgia	1 (6.7%)	0	0	0	1 (3.2%)	0
Myalgia	1 (6.7%)	1 (6.7%)	0	0	1 (3.2%)	1 (3.2%)
Respiratory, thoracic and mediastinal disorders	0	0	1 (6.2%)	1 (6.2%)	1 (3.2%)	1 (3.2%)
Interstitial lung disease	0	0	1 (6.2%)	1 (6.2%)	1 (3.2%)	1 (3.2%)

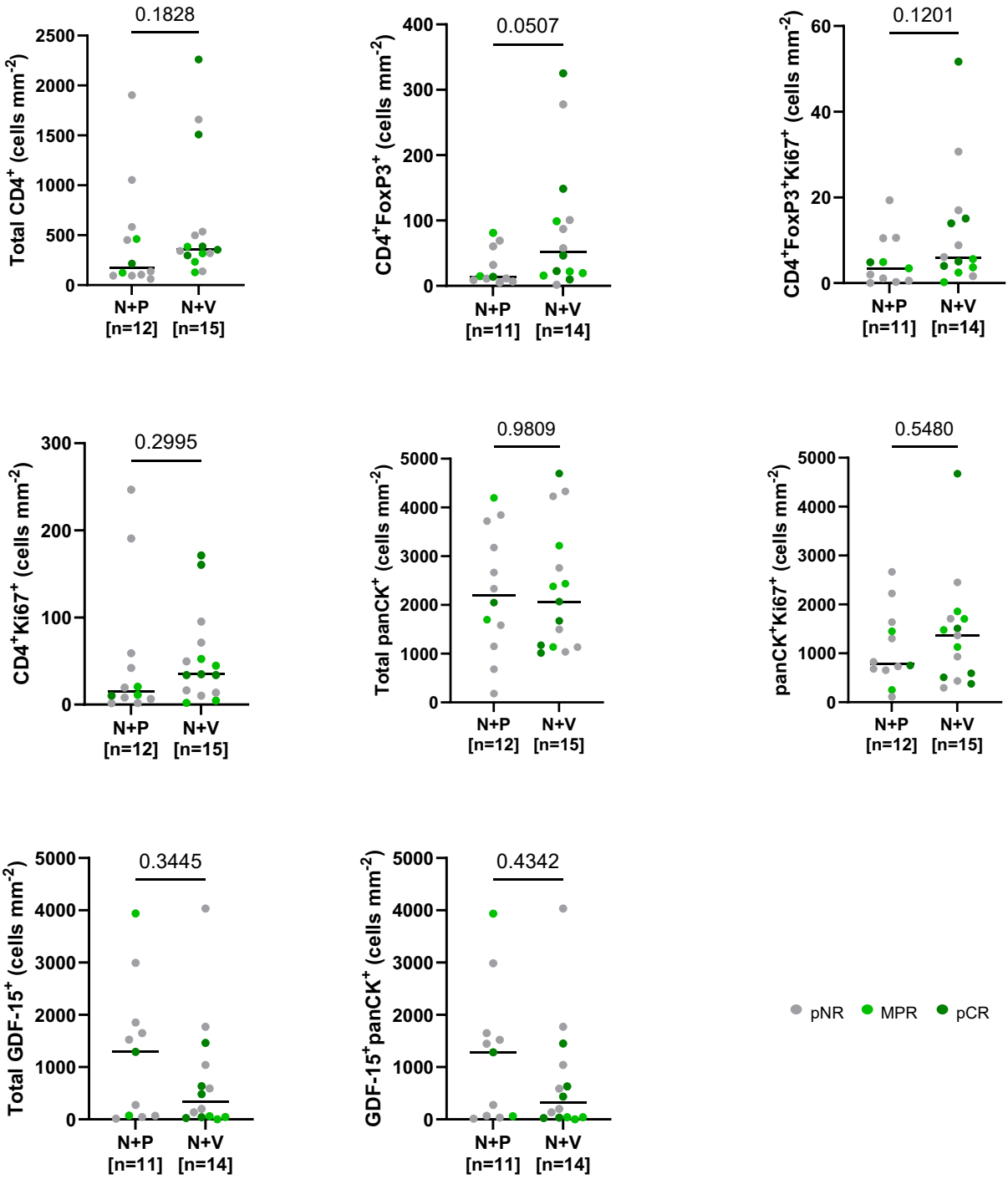
Abbreviations: N+P, nivolumab plus placebo; N+V, nivolumab plus visugromab. Adverse events by MedDRA Preferred Term (PT). Terms in bold are System Organ Class (SOC) terms.

https://doi.org/10.1038/s41591-026-04740-9



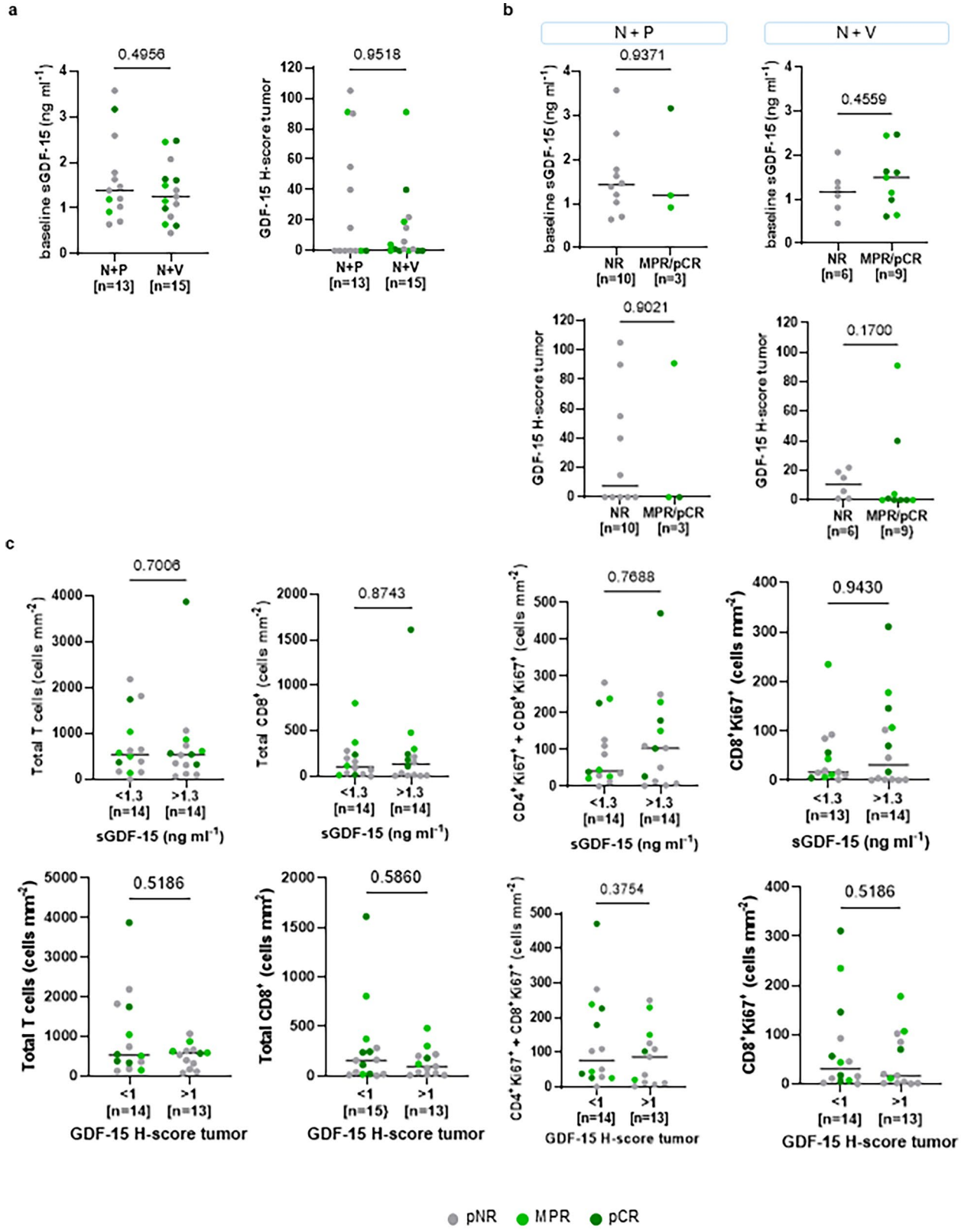
Extended Data Fig. 1 | Kaplan Meier estimates for event-free survival (EFS). Depicted is the ITT population for groups A (nivolumab plus placebo) and B (nivolumab plus visugromab).

https://doi.org/10.1038/s41591-026-04740-9



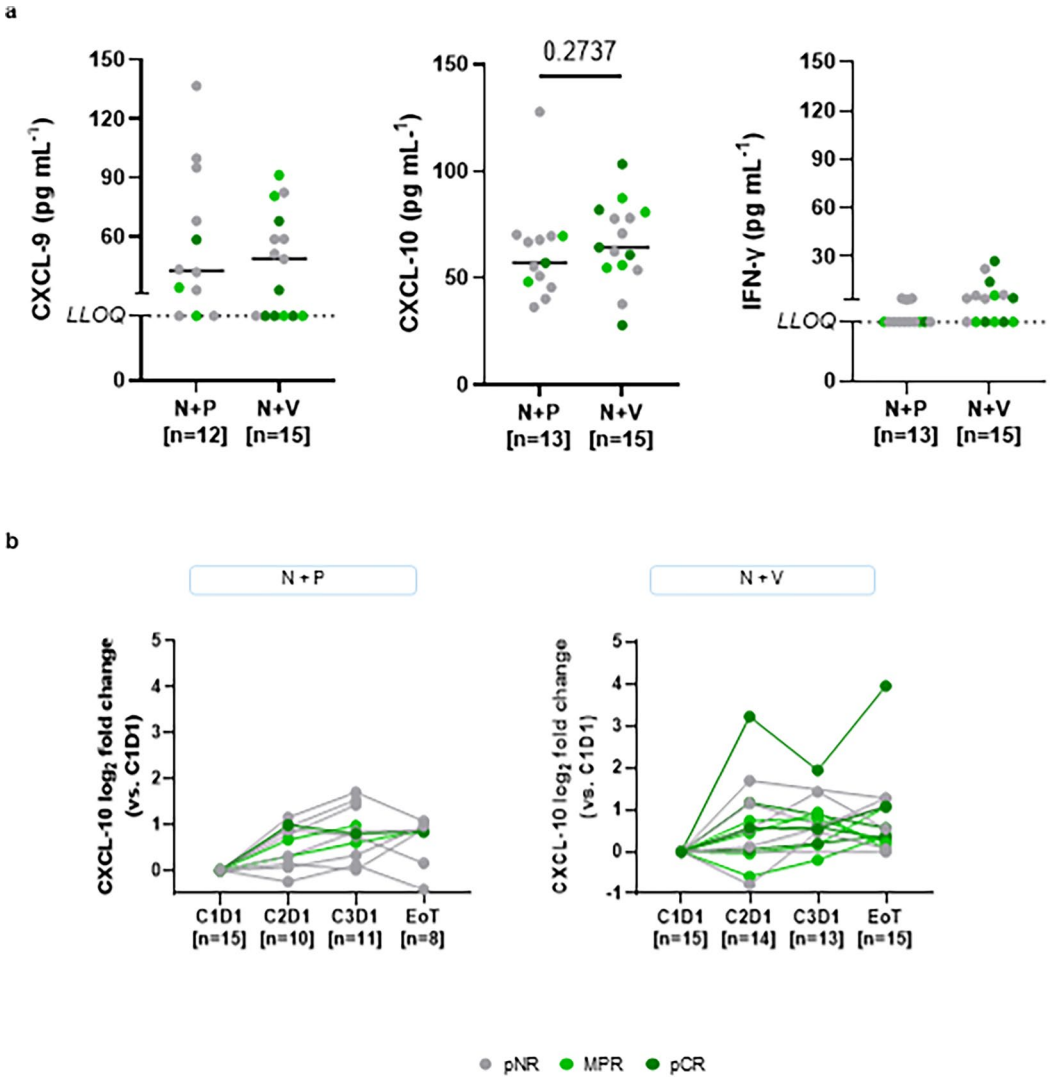
Extended Data Fig. 2 | Baseline multiplex immunofluorescence characterization of additional immune and tumor-cell populations. Baseline densities of $CD4^+$ T cells, regulatory T cells ($CD4^+FoxP3^+$), proliferating $CD4^+$ T cells ($CD4^+Ki67^+$), proliferating regulatory T cells ($CD4^+FoxP3^+Ki67^+$), total panCK$^+$ tumor cells, proliferating tumor cells (panCK$^+$Ki67$^+$), total GDF15$^+$ cells, and GDF15$^+$ tumor cells in tumors from the monotherapy (nivolumab plus placebo, N + P) and combination therapy (nivolumab plus visugromab, N + V) groups. Each data point represents one patient. Horizontal lines indicate medians. The distribution of individual observations is shown. Statistical comparisons were performed using two-sided Mann–Whitney U tests, as described for Fig. 4. mIF staining and analysis were performed once per patient specimen; each data point represents one patient.

https://doi.org/10.1038/s41591-026-04740-9



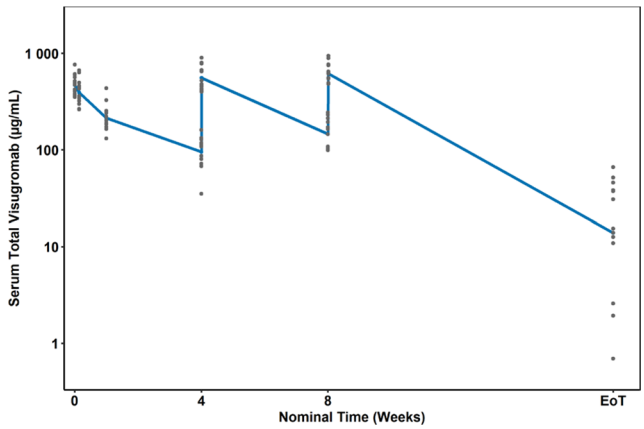
Extended Data Fig. 3 | Baseline circulating and intratumoral GDF-15 levels across treatment and pathologic response groups and their association with T-cell infiltration. (**a**) Baseline serum GDF-15 concentrations and intratumoral GDF-15 H-scores in the monotherapy and combination therapy groups. (**b**) Baseline serum GDF-15 concentrations and intratumoral GDF-15 H-scores stratified by pathologic response within each treatment group. (**c**) Baseline densities of total T cells, total $CD8^+$ T cells, proliferating CD4/CD8 T cells ($CD4^+Ki67^+/CD8^+Ki67^+$), and proliferating $CD8^+$ T cells ($CD8^+Ki67^+$) stratified by median serum GDF-15 concentration (**top**) or intratumoral GDF-15 H-score (**bottom**), with data pooled across treatment groups. Each data point represents one patient. Horizontal lines indicate medians. The distribution of individual observations is shown. Statistical comparisons were performed using two-sided Mann–Whitney U tests, as described for fig. 4. mIF staining and analysis were performed once per patient specimen; each data point represents one patient.

https://doi.org/10.1038/s41591-026-04740-9



Extended Data Fig. 4 | Baseline circulating cytokines and chemokines and longitudinal CXCL-10 dynamics. (**a**) Baseline circulating concentrations of CXCL9, CXCL10 and IFN-γ in the nivolumab plus placebo (N + P) and nivolumab plus visugromab (N + V) groups. Each data point represents one baseline serum sample from one individual patient. The horizontal dotted line indicates the lower limit of quantification (LLOQ). Horizontal lines indicate medians, and the distribution of individual observations is shown. Baseline comparisons between treatment groups were performed using two-sided Mann–Whitney U tests. (**b**) Longitudinal circulating CXCL10 concentrations measured at baseline (cycle 1 day 1, C1D1), cycle 2 day 1 (C2D1), cycle 3 day 1 (C3D1) and end of treatment (EoT). Data points represent individual patient measurements, and lines connect measurements obtained from the same patient at different time points. Panel **b** is presented descriptively; no formal statistical comparison of longitudinal changes was performed. Values below the LLOQ were assigned a value of LLOQ/2. *n* represents individual patients with an available measurement at the indicated time point. mIF staining and analysis were performed once per patient specimen; each data point represents one patient.

https://doi.org/10.1038/s41591-026-04740-9



Extended Data Fig. 5 | Visugromab serum concentrations over time. Observed total visugromab serum concentrations during treatment and at end-of-therapy (EoT). Individual observations and geometric mean concentrations are shown.

nature portfolio

Corresponding author(s): Necchi, Andrea

Last updated by author(s): Oct 2, 2026

Reporting Summary

Nature Portfolio wishes to improve the reproducibility of the work that we publish. This form provides structure for consistency and transparency in reporting. For further information on Nature Portfolio policies, see our Editorial Policies and the Editorial Policy Checklist.

Statistics

For all statistical analyses, confirm that the following items are present in the figure legend, table legend, main text, or Methods section.

n/a	Confirmed	
☐	☒	The exact sample size (*n*) for each experimental group/condition, given as a discrete number and unit of measurement
☐	☒	A statement on whether measurements were taken from distinct samples or whether the same sample was measured repeatedly
☐	☒	The statistical test(s) used AND whether they are one- or two-sided *Only common tests should be described solely by name; describe more complex techniques in the Methods section.*
☐	☒	A description of all covariates tested
☐	☒	A description of any assumptions or corrections, such as tests of normality and adjustment for multiple comparisons
☐	☒	A full description of the statistical parameters including central tendency (e.g. means) or other basic estimates (e.g. regression coefficient) AND variation (e.g. standard deviation) or associated estimates of uncertainty (e.g. confidence intervals)
☐	☒	For null hypothesis testing, the test statistic (e.g. *F*, *t*, *r*) with confidence intervals, effect sizes, degrees of freedom and *P* value noted *Give P values as exact values whenever suitable.*
☒	☐	For Bayesian analysis, information on the choice of priors and Markov chain Monte Carlo settings
☒	☐	For hierarchical and complex designs, identification of the appropriate level for tests and full reporting of outcomes
☐	☒	Estimates of effect sizes (e.g. Cohen's *d*, Pearson's *r*), indicating how they were calculated

Our web collection on statistics for biologists contains articles on many of the points above.

Software and code

Policy information about availability of computer code

Data collection	Clinical data collection via 'eCRF' (Medidata Rave EDC, v2020.1). IHC/IF image acquisiton was performed using Scanscope (console v102.0.7.5 and controller v102.0.8.60), Zen Blue (v3.1), PhenoImager HT imaging system (v1.1), Visiopharm (v2020.01.1, v2020.08.4) and inForm software (v2.5). IHC/IF image acquisiton was performed using PhenoImager HT imaging system (v1.1), and Visiopharm software (v2020.01.1, v2020.08.4).
Data analysis	Bar- and Kaplan-Meier plots were generated with R V4.6.1 and package Survminer V0.52. The swimmer plot was generated with SAS V9.4 Graph plotting and statistical analyis were performed with GraphPad Prism v11.0.0. Multiplex immunofluorescence staining was performed using a Leica Bond Rx platform with BOND-RX software v7.0.3.216. Whole-slide multispectral imaging was performed using an Akoya PhenoImager HT/Vectra Polaris platform with software v1.0.13, and digital image analysis was performed using Visiopharm v2021.09.2.11085. Pan-cytokeratin immunohistochemistry was performed using a Ventana Discovery Ultra platform with software v12.5 or higher. GDF-15 immunohistochemistry was performed using a Ventana BenchMark Ultra platform with software v12.3.1 and v12.5.4.

For manuscripts utilizing custom algorithms or software that are central to the research but not yet described in published literature, software must be made available to editors and reviewers. We strongly encourage code deposition in a community repository (e.g. GitHub). See the Nature Portfolio guidelines for submitting code & software for further information.

Data

Policy information about availability of data

All manuscripts must include a data availability statement. This statement should provide the following information, where applicable:

- Accession codes, unique identifiers, or web links for publicly available datasets
- A description of any restrictions on data availability
- For clinical datasets or third party data, please ensure that the statement adheres to our policy

Patient responses, demographic information, and safety outcomes, as well as IHC quantifications, serum analysis data and RNAseq signature scores are available within the paper, its supplementary information and provided as source data.

Normalized RNA sequencing data (TPM) from pan-cancer analyses of TCGA were obtained from http://firebrowse.org and together with related immune signatures, estimated immune cell fractions, as well as detailed information of selected indications (LUAD, LUSC, BLCA phenotypes) are available at zenodo (https://doi.org/10.5281/zenodo.13716226). Pathway analysis of gene expression data in patients is based on (Reactome) pathway information from ConsensusPathDB (http://cpdb.molgen.mpg.de/CPDB).

Research involving human participants, their data, or biological material

Policy information about studies with human participants or human data. See also policy information about sex, gender (identity/presentation), and sexual orientation and race, ethnicity and racism.

Reporting on sex and gender	Sex was recorded in this study as documented in the medical record and was used for descriptive purposes only; because of the small sample size of this prospective trial (n=31), no sex- or gender-based analyses were pre-specified, and none were performed.
Reporting on race, ethnicity, or other socially relevant groupings	There is no reporting on race, ethnicity or other socially relevant groupings in relation to this study which examines a new intervention in patients with bladder cancer.
Population characteristics	Population characteristics and demographics are fully described in Table 1 and Fig. 1 of the manuscript.
Recruitment	Patients were enrolled according to their diagnosis and disease stage and were required to fulfill all inclusion criteria and not meet any exclusion criteria accordingly. At the following highly experienced and specialized solid tumor clinical trial sites across Europe, patients were recruited and enrolled: - Department of Medical Oncology, IRCCS SAn Raffaele Hospital, Milan, Italy - Department of Oncology, Fondazione Policlinico Universitario Agostino Gemelli, Rome, Italy - Department of Medical Oncology, Fondazione IRCCS Istituto Nazionale dei Tumori, Milan, Italy - Division of Urology, Department of Surgical Sciences, San Giovanni Battista Hospital, Turin, Italy. For the recruiting sites, competitive recruitment applied and enrolment numbers varied between sites depending on availability of eligible patients. Due to the clearly defined inclusion and exclusion criteria together with the large number of clinical trial sites across Europe, no selection bias is evident. Patients who were offered participation in the clinical trial were carefully informed about alternative treatment options. Patients were provided copies of the study informed consent document and were fully aware of risks prior to trial enrollment. As patients needed to fulfill eligibility criteria of the trial, this could have caused selection bias.
Ethics oversight	The regulatory authority in Italy (Agenzia Italiana del Farmaco (AIFA), Italian Medicines Agency) and the ethics committee in charge of the clinical trial (Lombardy Territorial Ethics Committee 1 (Comitato Etico Territoriale Lombardia 1)) approved the study following applicable rules and regulations.

Note that full information on the approval of the study protocol must also be provided in the manuscript.

Field-specific reporting

Please select the one below that is the best fit for your research. If you are not sure, read the appropriate sections before making your selection.

☒ Life sciences ☐ Behavioural & social sciences ☐ Ecological, evolutionary & environmental sciences

For a reference copy of the document with all sections, see nature.com/documents/nr-reporting-summary-flat.pdf

Life sciences study design

All studies must disclose on these points even when the disclosure is negative.

Sample size	The study was conducted as an exploratory, stratified phase 2 trial. No formal sample size calculation was performed and no hypothesis was tested; the trial was not powered to detect a statistically significant difference between treatment groups, and all comparisons between groups are exploratory.

	Statistical design of phase 2a is described in the methods section of the manuscript accordingly.
Data exclusions	No data exclusions occurred.
Replication	Clinical trial results can not be replicated.
Randomization	The reported study is a prospectively planned phase 2 study with sequential treatment allocation of patients to four strata (covariate-stratified, parallel group comparative study). Patients inside each stratum were then sequentially (1:1) allocated to both treatment groups.
Blinding	The reported study was single-blinded (participants, but not investigators).

Reporting for specific materials, systems and methods

We require information from authors about some types of materials, experimental systems and methods used in many studies. Here, indicate whether each material, system or method listed is relevant to your study. If you are not sure if a list item applies to your research, read the appropriate section before selecting a response.

Materials & experimental systems

n/a	Involved in the study
☐	☒ Antibodies
☒	☐ Eukaryotic cell lines
☒	☐ Palaeontology and archaeology
☒	☐ Animals and other organisms
☐	☒ Clinical data
☒	☐ Dual use research of concern
☒	☐ Plants

Methods

n/a	Involved in the study
☒	☐ ChIP-seq
☒	☐ Flow cytometry
☒	☐ MRI-based neuroimaging

Antibodies

Antibodies used

GDF-15/TME multiplex immunofluorescence 6+1 panel
- Anti-CD4, clone F7.2.38, rabbit monoclonal antibody, Cell Marque, catalogue no. 104R-14.
- Anti-CD8, clone C8/144B, mouse monoclonal antibody, Agilent Technologies, catalogue no. M7103.
- Anti-Ki-67, clone MIB-1, mouse monoclonal antibody, Agilent Technologies, catalogue no. M7240.
- Anti-FoxP3, clone SP97, rabbit monoclonal antibody, Abcam, catalogue no. ab99963.
- Anti-PD-L1, clone SP263, rabbit monoclonal antibody, Roche Diagnostics, catalogue no. 741-4905.
- Anti-GDF-15, rabbit polyclonal antibody, Sigma-Aldrich, catalogue no. HPA011191.
- Anti-pan-cytokeratin, clones AE1/AE3, mouse monoclonal antibodies, Agilent Technologies, catalogue no. M3515. Pan-cytokeratin immunohistochemistry was performed subsequently on the same slide.

PD-L1 immunohistochemistry
- Anti-PD-L1, clone SP263, rabbit monoclonal antibody, Roche Diagnostics, catalogue no. 790-4905.
- Rabbit IgG monoclonal isotype control, Roche Diagnostics, catalogue no. 790-4795.

GDF-15 immunohistochemistry
- Anti-GDF-15, rabbit polyclonal antibody, Sigma-Aldrich, catalogue no. HPA011191.
- Anti-GDF-15 antibody binding was visualised using the Ventana OptiView Universal DAB Detection Kit, Roche Diagnostics, catalogue no. 760-700, containing secondary horseradish peroxidase-conjugated antibody reagents.

Validation

The GDF-15/TME 6+1 multiplex immunofluorescence assay was established and validated at research-use-only level for exploratory testing of human formalin-fixed, paraffin-embedded urinary bladder cancer tissue. Staining quality was assessed using pre-tested on-slide control tissue and predefined marker-specific internal controls in the patient tissue. If one or more markers showed no, insufficient, non-specific or implausible staining, the affected markers were excluded from evaluation, while markers meeting the predefined quality criteria remained evaluable. Digitally scanned whole-slide images were analysed using validated Visiopharm image-analysis algorithms under pathologist oversight.

For the PD-L1 and GDF-15 immunohistochemistry assays, a batch control including an isotype control was included for each staining run, and an isotype control was included for each patient sample. PD-L1 and GDF-15 staining were evaluated by board-certified pathologists.

Clinical data

Policy information about clinical studies

All manuscripts should comply with the ICMJE guidelines for publication of clinical research and a completed CONSORT checklist must be included with all submissions.

Clinical trial registration	NCT06059547; EudraCT Number 2022-002816-22
Study protocol	Study protocol can be accessed at https://www.clinicaltrialsregister.eu/ctr-search/trial/2022-002816-22/IT and was provided as redacted version to Nature Medicine.
Data collection	Data were collected at the following 4 clinical trial sites in Italy: -- Department of Medical Oncology, IRCCS SAn Raffaele Hospital, Milan, Italy - Department of Oncology, Fondazione Policlinico Universitario Agostino Gemelli, Rome, Italy - Department of Medical Oncology, Fondazione IRCCS Istituto Nazionale dei Tumori, Milan, Italy - Division of Urology, Department of Surgical Sciences, San Giovanni Battista Hospital, Turin, Italy. Patient enrolment and trial participation lasted from 09/2023 to 03/2026. Data collection started in 09/2023 and is ongoing (follow-up period).
Outcomes	Outcomes are defined in the clinical study protocol and in the methods section of the manuscript (response and safety assessment). Assessment of additional secondary endpoints including pharmacokinetics and -dynamics are described in the methods section of the manuscript.

Plants

Seed stocks	*Report on the source of all seed stocks or other plant material used. If applicable, state the seed stock centre and catalogue number. If plant specimens were collected from the field, describe the collection location, date and sampling procedures.*
Novel plant genotypes	*Describe the methods by which all novel plant genotypes were produced. This includes those generated by transgenic approaches, gene editing, chemical/radiation-based mutagenesis and hybridization. For transgenic lines, describe the transformation method, the number of independent lines analyzed and the generation upon which experiments were performed. For gene-edited lines, describe the editor used, the endogenous sequence targeted for editing, the targeting guide RNA sequence (if applicable) and how the editor was applied.*
Authentication	*Describe any authentication procedures for each seed stock used or novel genotype generated. Describe any experiments used to assess the effect of a mutation and, where applicable, how potential secondary effects (e.g. second site T-DNA insertions, mosiacism, off-target gene editing) were examined.*